2011

Structural and Functional Alteration of Full Length PPARα and LXRα by Fatty Acids and their Thioesters

Madhumitha Balanarasimha
Wright State University

STRUCTURAL AND FUNCTIONAL ALTERATION OF FULL LENGTH PPARα AND LXRα BY FATTY ACIDS AND THEIR THIOESTERS

A thesis submitted in partial fulfillment
of the requirements for the degree of
Master of Science

By

MADHUMITHA BALANARASIMHA
M.Sc. Biotechnology, Bangalore University, India, 2006

2011
Wright State University

WRIGHT STATE UNIVERSITY

SCHOOL OF GRADUATE STUDIES

November 4, 2011

I HEREBY RECOMMEND THAT THE THESIS PREPARED UNDER MY SUPERVISION BY Madhumitha Balanarasimha ENTITLED Structural and Functional Alteration of Full Length PPARα and LXRα by Fatty Acids and their Thioesters BE ACCEPTED IN PARTIAL FULFILLMENT OF THE REQUIREMENTS FOR THE DEGREE OF Master of Science.

_____

Heather A Hostetler, Ph.D.
Thesis Director

_____

Steven Berberich, Ph.D., Chair
Department of Biochemistry and Molecular Biology

Committee on
Final Examination

_____

Heather A Hostetler, Ph.D.

_____

Steven Berberich, Ph.D.

_____

Lawrence J. Prochaska, Ph.D.

_____

Andrew Hsu, Ph.D.
Dean, School of Graduate Studies

ABSTRACT

Balanarasimha, Madhumitha. M.S., Department of Biochemistry and Molecular Biology, Wright State University, 2011. Structural and Functional Alteration of Full Length PPARα and LXRα by Fatty Acids and their Thioesters.

Peroxisome proliferator-activated receptors (PPAR) and liver X receptors (LXR) are known to play important roles in fatty acid metabolism, interact with each other, and function as heterodimeric partners. Although previous studies indicate that PPARα is activated by long chain fatty acyl-CoA thioesters (LCFA-CoA) and polyunsaturated fatty acids, little is known about the effects of these ligands on the function or interaction of PPARα and LXRα. In this study, hPPARα and hLXRα were shown to directly interact by circular dichroism, fluorescent binding assays, and co-immunoprecipitation. Further experiments suggested that although fatty acids resulted in small structural changes, they significantly altered binding affinities; while LCFA-CoAs decreased the binding affinities, no observable trend was seen with respect to the number of carbon atoms or bonds. In addition, transactivation assays in the presence of certain fatty acids suggested that the combination of PPARα and LXRα increased the activity of the PPARα regulated gene – ACOX, while downregulating the LXRα regulated gene SREBP. As high levels of fatty acids are associated with certain metabolic disorders and also serve as natural ligands for PPARα, changes in structure and/or interaction between PPARα and LXRα may have significant effects on the normal functioning of a cell.

TABLE OF CONTENTS

LIST OF FIGURES

LIST OF TABLES

TABLE **Page**

ACKNOWLEDGEMENTS

I would like to first thank my advisor Dr. Heather. A. Hostetler for believing in me and giving me the opportunity to work in her lab, for her patience, encouragement, support and guidance throughout my thesis research.

I would also like to thank my committee members, Dr. Prochaska and Dr. Berberich for all their time, help and support with my thesis.

I sincerely thank my parents, Balanarasimha and Padmavathy and my husband, Arun Ranjan for their unconditional love, invaluable support and motivation.

Last but not the least; I would like to thank all my lab members and friends for believing in me and being there for me when I needed them.

I. INTRODUCTION

The rising prevalence of diabetes and some of its related diseases, such as cardiovascular disease and stroke, are of growing concern. According to statistics from the Center for Disease Control, diabetes, stroke and cardiovascular diseases are among the top ten causes for death in the United States [1]. Records from the National Institute of Diabetes and Digestive and Kidney Diseases state that diabetes affects about 9% of the U.S. population of all ages, and also shows that at least two out of three people with diabetes suffer from a heart attack or stroke [2] which is commonly caused due to elevated levels of lipids and accumulation of fats. The tight regulation by certain proteins/nuclear-receptors/transcription-factors that regulate genes involved in fatty acids and lipid metabolism are of utmost importance in maintaining energy homeostasis, thereby preventing or controlling such situations.

Nuclear Receptors

Nuclear receptors are a class of ligand-activated transcription factors found in the interior of the cell that are able to recognize and regulate the expression of genes involved in energy homeostasis, metabolism, development and reproduction in response to molecules such as retinoid-, steroid- and thyroid-hormones [3, 4]. In addition to these hormones, a number of other molecules such as sugars [5], amino acids, lipids, and bile

acids also act as ligands and regulate the transcription of such genes [6] [7]. While a majority of the ligands have been identified for these nuclear receptors, some of the endogenous ligands are still unknown and therefore these receptors are called orphan receptors [8].

The initial discoveries of several nuclear receptors in the late 1980s including retinoid X receptor (RXR) by Ron Evan's group [9] and 9-cis retinoic acid receptor (RAR) by Pierre Chambon's group [10], followed by other receptors such as PPAR, LXR, and farsenoid x receptor (FXR), can be attributed to the emergence of this class of orphan nuclear receptors, which paved the way to unravel some of the novel ligands now known [11]. Nuclear receptors were originally classified based on their ability to bind to DNA and ligands. However, a more recent classification is based on sequence similarity classifying the receptors into six subfamilies: NR1 to NR6 with several subgroups among them [12]. Nuclear receptors have the ability to bind to specific sites on DNA called half sites of the hormone response elements (HRE) as monomers, homodimers or heterodimers [13]. The HREs can be further classified into direct-, indirect- and inverted-repeats [14] located in the 5' region of the target genes commonly closer to the promoter, and are composed of a set of repeating nucleotide sequences that are separated by either one or more nucleotides [12]. While some of the receptors, such as PPAR, LXR, and RXR, are activated upon ligand binding, a few receptors such as the constitutive androsterone receptor (CAR) are ligand-independent and are constitutively active [11]. However in the case of a ligand-dependent nuclear receptor, ligand binding

either upregulates or downregulates the target genes leading to activation or inactivation of a given pathway.

Structure of Nuclear Receptors

Nuclear receptors are generally composed of 5 motifs: an NH_2-terminal A/B domain, a DNA binding domain (DBD), a hinge region, a ligand binding domain (LBD) and a C-terminal domain [4].

The NH_2-terminal domain varies among species with respect to both size and sequence and displays specificity with reference to the species they identify and sequences that they bind to [15]. The A/B domain, which also contains a ligand-independent activation function (AF-1), is responsible for the specificity among the different isoforms of a nuclear receptor and plays a key role in activation of these receptors in either a ligand-dependent or ligand-independent fashion [15]. Adjacent to this A/B domain is the conserved DBD which aids in the binding of the receptor to specific sites on the DNA called the HRE. The DBD is composed of two zinc-fingers bonded to two pairs of cysteine residues [16]; one of which is located in the proximal-box (P-box) responsible for recognition of sites on the HRE and binding them with high affinity; and the second in the distal-box (D-box) that mediates dimerization of receptors. Upon recognition and binding to the DNA, these receptors can function either as activators (i.e. in transcribing the genes that the nucleotide codes for) or as repressors of

the genes. The region between the DBD and the LBD acts as a hinge, and allows changes in conformation upon ligand binding. The hinge region is also thought to have protein-protein interaction sites; however the actual function is still unknown.

The LBD, which is mainly comprised of 11 to 13 alpha helices, forms a large hydrophobic pocket where it accommodates the ligand and undergoes conformational changes after being bound [17]. While studies have shown that the LBDs of most receptors are similar structurally, the sizes vary among receptors. For example; each of the three isotypes of PPAR have a large LBD pocket that ranges between 1300-1400 $Å^3$ [17-20] which accommodates a variety of natural endogenous, as well as synthetic ligands, while the LBD of LXR isotypes can accommodate ligands only as big as 400 $Å^3$ [21]. Finally, the other end of the receptor, which is the C-terminal region, also called the F domain, contains an activation domain called the activation factor-2 (AF-2), which is responsible for ligand dependent activation and confers ligand specificity.

PPAR

PPARs belong to the class of ligand activated transcription factors of the NR1C subfamily of receptors [22], similar to the vitamin D receptor, thyroid receptor and retinoic acid receptor that also belong to the NR1 subfamily. While the phenomenon of peroxisome proliferation was first seen in the 1960's as a response to drugs such as fibrates in rodents [23], successful cloning of the PPAR gene from a mouse liver did not

occur until 1990 [24]. Since the discovery of this receptor that resulted in peroxisome proliferation, now known as PPARα [25], two other isotypes – PPARβ and PPARγ were also discovered and cloned by the Wahli group [24]. However, the nomenclature for the two isotypes, PPARβ and PPARγ, can be considered as a misnomer since peroxisome proliferation is not seen in either of these two subtypes [25, 26]. The PPAR isotypes (α, β and γ) are expressed in different tissues based on their functions. For example; PPARα is expressed most predominantly in the liver, heart and kidneys that require a lot of energy for their metabolic functioning. Further, PPARγ is expressed in white adipose tissue, spleen and large intestine and the beta isotype is found ubiquitously.

PPARs play an important role in a number of physiological functions, including metabolism of fats and sugars such as glucose [27, 28], cellular proliferation and differentiation [29], and also in inflammation [30]. Therefore, PPARs are implicated in a number of disorders including obesity, diabetes, cardiovascular diseases, atherosclerosis and cancer [31]. Many endogenous and exogenous ligands play a role in activating the receptor, which in turn regulates its' target genes. For example, drugs such as fibrates, roziglitazones and thiazolidinedione are exogenous ligands of PPARγ [32, 33], whereas naturally occurring fatty acids, eicosanoids and also fibrates act as PPARα ligands [34]. Upon ligand activation, PPARα regulates genes including those coding for acyl-CoA oxidase (ACOX), liver-fatty acid binding protein (L-FABP) and carnitine palmitoyl transferase (CPT1A), which function in fatty acid metabolism, transport of LCFAs in liver and transport of LCFAs across the mitochondrial membrane respectively.

As any other nuclear receptor, PPARs also have an N-terminal A/B domain that is highly species specific and perhaps account for the differences that exist among the different species. For example, peroxisome proliferation seen in rodents as a response to fibrates is not seen in humans [35]. PPARs are known to heterodimerize with other receptors such as RXR [36] and thyroid receptor (TR) [37] at the LBD and DBD domain [38] to form an active complex which then binds to the DNA to control gene expression by interacting with specific sites on the DNA response elements such as peroxisome proliferator response elements (PPRE) located upstream of target genes. In addition to dimerization, binding of ligands such as fibrates and long chain fatty acids that cause a change in the conformation, also play a role in the activation of the nuclear receptor complex [39]. For example, PPARα activation can regulate the function of ACOX gene coding for the protein – acyl CoA oxidase, which is one of the first enzymes of fatty acid beta oxidation. ACOX aids in the conversion of acyl-CoA to trans-Δ2-enoyl-CoA [40].

LXR

Liver X receptor, commonly known as the cholesterol sensor [41, 42], is involved in regulating transport and metabolism of sterols and fatty acids and therefore plays a critical role in lipid homeostasis. The two isotypes of LXRs that have been identified - LXRα and LXRβ, also belong to the NR1H family of nuclear receptors and are known to share a sequence similarity of about 77% in both the DBD as well as the LBD [42, 43].

While compounds such as oxysterols, oxidized derivatives of cholesterol, were first identified as potent ligands, several other cholesterol derivatives including 24(*S*)-hydroxycholesterol, 22(*R*)-hydroxycholesterol and 24(*S*),25-epoxycholesterol were also found to serve as potent ligands of LXRα [44, 45]. While LXRα is predominantly expressed in liver, intestine and adipose tissue [46], the beta form lacks tissue specificity and is expressed in almost all tissues [47, 48].

LXRs are also involved in glucose [49] and cholesterol homeostasis [50], inflammation [51], and atherosclerosis [42]. LXRs can form heterodimers with other nuclear receptors such as RXR and bind to response elements known as Liver X receptor response elements (LXRE) to regulate a number of genes such as the sterol regulatory element binding protein (SREBP) [52, 53], fatty acyl synthase (FAS) and glucose transporter (GLUT1). As the name suggests, SREBP codes for a binding protein that regulates the synthesis of sterols (cholesterols) and fatty acids, and maintains the levels of intracellular lipids. Thus LXR, like PPAR, determines the fate of the molecules to which it binds.

Why PPARα and LXRα??

PPARα and LXRα regulate transcription of genes involved in metabolism, and therefore their normal functioning is important in maintaining energy homeostasis. PPARα binding to fatty acids, fatty acyl thioesters, and eicosanoids facilitates fatty acid

uptake, transport and oxidation. LXRα binds oxysterols and endogenous cholesterol derivatives and regulates cholesterol transport, genesis and degradation. Both PPARα and LXRα function as heterodimeric partners with the retinoid X receptor alpha (RXRα) in order to control gene regulation. Previous studies have suggested that PPARα and LXRα themselves can function as heterodimeric partners [54], but the significance of this finding is unclear. Two separate studies by Ide et al have shown that a crosstalk exists between PPARα and LXRα in regulating fatty acid metabolism. The study suggests that PPARs suppress the activity of SREBP-1c gene by inhibiting the signaling pathway of LXR and that LXRs inhibits PPAR signaling pathway thus suppressing its activity [54, 55]. However, it is not known whether the inhibition occurs due to a direct or an indirect interaction between the two nuclear receptors.

Also, it is not known if fatty acids or fatty acyl thioesters promote or inhibit PPARα and LXRα heterodimer formation. Most studies involving these receptors have used either truncated or tagged proteins, and therefore not much is known about the activity and effects of full-length proteins. Moreover, the effects of nuclear receptor activation by ligands differ among species (eg. peroxisome proliferation induced by PPARα agonists are only seen in rodents and not in humans) and very few studies have utilized full-length human version of these receptors. Any change in the receptor's structure can result in a change of its function leading to metabolic disorders such as diabetes, obesity, atherosclerosis and cardiovascular diseases. Thus, it becomes imperative to study the effects of various putative ligands on the human, full-length

versions of these receptors. The objective of this study was to look at the effects of saturated and unsaturated fatty acids and fatty acyl thioester derivatives on the interaction of human PPARα and LXRα.

II. GOALS AND HYPOTHESES

The three goals of this study were: firstly, to examine whether or not full-length hPPARα and hLXRα directly interact with each other; secondly to study the effects of LCFAs and LCFA-CoAs on the interaction of hPPARα and hLXRα; and finally to study the effects of LCFAs and LCFA-CoAs on the function of hPPARα and hLXRα regulated genes.

In order to test the goals, the following hypotheses were made. The first being, full length recombinant hPPARα and hLXRα directly interact with high affinity; secondly fatty acids and/or fatty acyl-CoA affect the interaction between the proteins, and finally, fatty acids and/or fatty acyl-CoA that affect the interaction will have an effect on the activity of the two proteins.

III. MATERIALS AND METHODS

Protein Expression in Bacteria

Full-length, tagged recombinant human PPARα and LXRα proteins were expressed in *Escherichia coli,* purified using affinity chromatography, and tags were removed by on-column cleavage. The plasmids encoding the recombinant proteins, 417 amino acid long PPARα and 453 amino acid long LXRα were individually cloned into separate pGEX-6-P3 bacterial expression vectors which were modified to include an N-terminal 6X histidine tag between the start codon and the Glutathione S transferase (GST) tag. These plasmids were produced in the Hostetler lab by Dr. S. Dean Rider, Jr. Growing conditions were first tested in order to optimize the purity and yield of the two proteins. Rosetta cells derived from a BL21 strain (Novagen, Philadelphia , PA) were transfected with the ampicillin-resistant plasmid pHH55 (Figure 1A), which codes for full-length His_6-GST tagged- hPPARα was used to express the protein, and a DNAK mutant derived from a K12 strain (JW0013, E. coli Stock Center) transfected with the ampicillin-resistant plasmid pHH3-1 (Figure 1B) was used to express full-length hLXRα.

For hPPARα, an overnight culture was grown in 100ml Luria Bertani (LB) media (Becton Dickson) containing 0.1mg/ml ampicillin, 0.2mg/ml chloramphenicol and 10% glucose at 30^{o}C and 200 rpm. The following day, this 100ml overnight culture was subcultured into 1L of LB at 37^{o}C for up to 3 hours until an OD_{600} of 1.5-1.8 was

obtained. After the desired OD was reached, protein expression was induced with 0.1M IPTG for 4 hours at 16^{o}C. The cells were then pelleted using an Avanti-J26 XPI centrifuge at 8500rpm for 10minutes at 4^{o}C, and 100mM PMSF was added to the pellet to stop the action of proteases.

For hLXRα, an overnight 40 ml LB (Sigma Aldrich) culture was grown at 37^{o}C and 175 rpm in the presence of 0.1mg/ml ampicillin, 0.2mg/ml chloramphenicol and 10% glucose. The overnight culture was then subcultured into 1L of pre-warmed LB media and grown for 2 hours at 30^{o}C at 200 rpm, following which the temperature was turned down to 16^{o}C and continued to grow for 2 more hours. The culture was then induced with 0.1M IPTG for 4 hours at 16^{o}C and pelleted using an Avanti-J26 XPI centrifuge at 8500 rpm for 10minutes at 4^{o}C. Again, 100mM PMSF was added to the pellet to stop the action of proteases. The pellets were then stored in -80^{o}C for further protein purification.

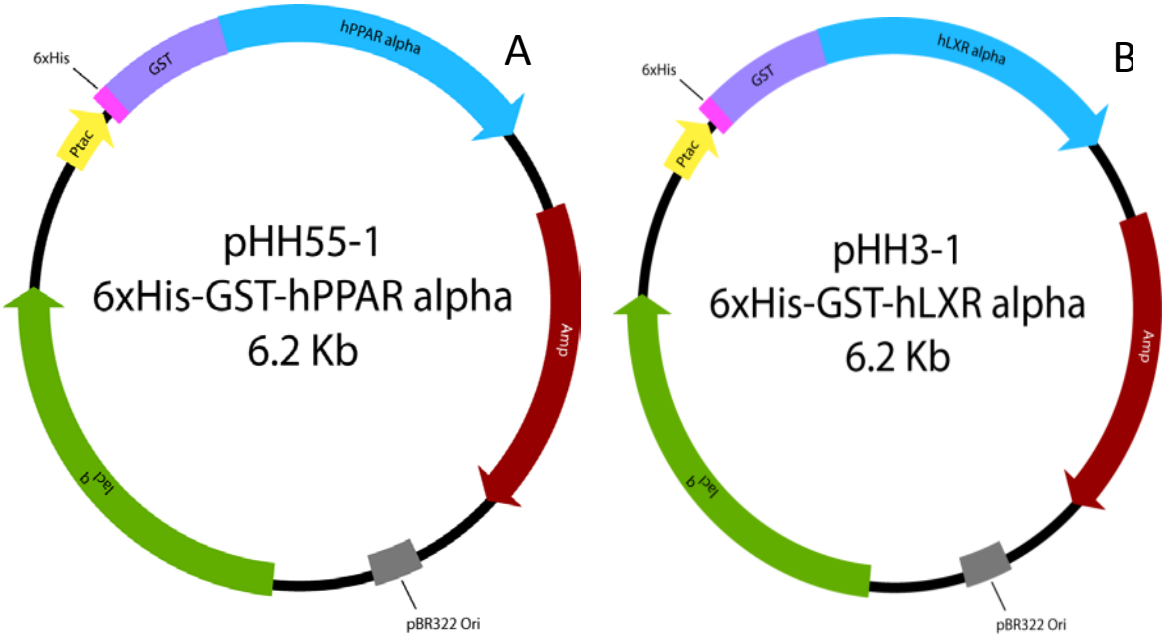

FIGURE 1: Schematic representation of plasmid DNA coding for full-length hPPARα and hLXRα with 6His-GST tag. (A) The cDNA encoding the complete hPPARα with the amino acids 1-473 was cloned into a pGEX-6-P3 bacterial expression vector which was modified to include an N-terminal 6X histidine tag between the start codon and the Glutathione S transferase (GST) tag. This construct was then expressed in the BL21 Rosetta strain of *Escherichia coli* and purified by affinity chromatography using a GST affinity column. **(B)** The cDNA encoding the complete hLXRα with 453 amino acids was cloned into a pGEX-6-P3 bacterial expression vector which was modified to include an N-terminal 6X histidine tag between the start codon and the Glutathione S transferase (GST) tag. This construct was then expressed in the DNAK mutant strain of *Escherichia coli* and purified by affinity chromatography using a GST affinity column.

Protein Purification using Affinity Chromatography

On the day of purification, the pellets were resuspended in 10mls of 2X L&C buffer (40mM Tris, pH 8.0, 0.35mM NaCl and 20% glycerol) [56] SDS-PAGE analysis was containing 1mM DTT and 2mM EDTA and 10mls 2X protease inhibitor SIGMAFAST™ protease inhibitor cocktail tablet, EDTA-free (Sigma-Aldrich, St. Louis, MO) resuspended in 2X L&C buffer. The cell suspension was sonicated on ice six times for 30 seconds, with 30 second intervals between each sonication, at an amplitude of 50% with a Sonic Dismembrator (Fischer Scientific). The cell debris was pelleted by centrifugation using an Avanti-J26 XPI centrifuge at 10,000 rpm for 20 minutes.

The cell lysate obtained after pelleting the cell debris was completely circulated in the affinity chromatography column with glutathione sepharose resin at the flow rate of 0.1ml per minute and was washed three times; first with 2mls of 1X L&C buffer (20mM Tris, pH 8.0, 0.175mM NaCl and 10% glycerol), followed by 5mls of ATP wash buffer (2X L&C buffer, 10mM ATP and 50mM $MgCl_2$), and finally with 10mls of 1X L&C buffer (containing 1mM DTT and 2mM EDTA) in order to remove any unbound protein from the column. Following the three washes, a PreScission protease mix (1 ml 1X L&C containing 1mM DTT and 0.5mM EDTA and 120µg protease) was circulated through the column for 4 hours at $4^{o}C$, after which the full-length untagged recombinant protein was eluted. Additional elutions of 1ml (of 1X L&C containing DTT and EDTA) were collected to completely remove any remaining cut protein from the column.

Protein Estimation

The protein content in the elute was analyzed using both the Bradford assay and the molar extinction coefficient, which defines the strength of absorption of light at a given wavelength by the substance, based on its molar concentration. The sample (5µl) was mixed with 195µl of Bradford reagent (Bio-Rad Inc.) and standards were set up using IgG protein standards (Sigma Aldrich), ranging from 0.1mg/ml to 1mg/ml of IgG. The absorbance was read at 595 nm using a plate reader in spectrophotometer (SAFIRE^2 DECAN), a standard curve was generated using the IgG concentration, and protein concentrations were calculated by extrapolating the absorbance values of the samples against the standard curve of IgG. The concentration of the protein-dye complex was calculated by factoring in the protein concentration and molar extinction coefficient of the protein and the dilution factor.

SDS-PAGE & Western Blot Analysis

SDS-PAGE analysis was conducted following protein estimation, for separation and visualization of the protein band corresponding to its molecular weight of about 50kDa (for both hPPARα and hLXRα). The protein elute (10µg) was mixed with 2X sample buffer (10%SDS, 2M Tris, pH6.8, 1.2% bromophenol blue, 10% glycerol), heated at 90^{o}C for 3 minutes and loaded onto a 12% SDS-PAGE gel using standard techniques. Prestained Benchmark Protein markers (Invitrogen) were loaded together with the protein

samples and the gel was run at constant amps for 60 minutes. Following the separation using SDS-PAGE, the gel was stained using Coomassie blue, destained in 7.5% acetic acid and visualized using the Fujifilm LAS 4000 imaging system. However, for western blot analysis, the resolved gel was directly used to transfer the proteins onto nitrocellulose membrane using a BioRad electrotrans blot apparatus overnight at 30 volts and 4^{o}C per the manufacturer's recommendations. Following the transfer, the blots were blocked with 3% BSA in TBST overnight at 4^{o}C and later incubated with primary antibodies using anti-mouse monoclonal PPARα antibody (MA1-822, ThermoScientific) and anti-goat polyclonal LXRα (PA1-330, ThermoScientific) at a concentration of 1µg/750µl in 1% BSA in TBST for PPARα and LXRα respectively for 1 hour at room temperature on a rocker. After treating with primary antibodies, the blots were washed thrice using TBST for 5 minutes and then treated with respective secondary antibodies at a concentration of 1µg/10ml in 1% BSA in TBST for 1 hour at room temperature. The blots were again washed thrice with TBST with 5 minute incubation each time in order to remove any unbound antibody. Finally, a 15 minute wash with TBS was performed, after which the blots were developed using alkaline phosphatase reagent and imaged using the Fuji Film LAS-4000 imaging system.

Circular Dichroism

A JASCO-815 spectropolarimeter was used to analyze the structure of hPPARα and hLXRα proteins individually, and also as a mixture to determine any possible

interaction between the two proteins as previously described for mouse PPARα by Hostetler et al [57]. Further, circular dichroic spectra of the two proteins in the presence and absence of both saturated and unsaturated fatty acids and their CoA thioesters were taken to determine their effects on the structure of hPPARα and hLXRα. The fatty acids Palmitic acid (C16:0), Oleic acid (C18:1), Linoleic acid (C18:2) and Eicosapentaenoic acid (EPA) (C20:5) and their CoA thioesters; Palmitoyl CoA (C16:0-CoA), Oleoyl CoA (C18:1-CoA), Linoleoyl CoA (C18:2) and EPA-CoA (C20:5-CoA) were used in this experiment. An average of 5 scans at the rate of 50nm/min was acquired in order to account for any errors and a minimum of three repetitions were conducted for accuracy, with a D.I.T of 1 second and a bandwidth of 2nm. While stock solutions of each fatty acid were diluted in 50% ethanol, the final ethanol concentration in each reaction was less than 0.05%. The protein sample was suspended in a low salt buffer (0.5mM HEPES containing 0.005mM EDTA, 5mM KCl and 0.04% glycerol) to ensure that the absorbance due to salt does not interfere with the signal from the proteins. Appropriate controls with dialysis buffer and ethanol were also run to account for any changes caused due to salt and ethanol. A far UV scan from 260nm to 185nm was read to determine the secondary structure of the proteins**.** For optimum absorbance readings, both hPPARα and hLXRα were used at an amino acid concentration of 0.0002M. For this amino acid molarity, 0.42μM hPPARα, 0.44μM hLXRα was used in absence and combination with 0.5μM fatty acids and their CoA thioesters when the spectra of two proteins were read individually with the ligands. However, when the spectra of a mixture of hPPARα and hLXRα with the ligands were read, the amino acid concentrations were adjusted to a total

of 0.0002M by using exactly half the concentration (i.e. 0.21μM hPPARα, 0.22μM hLXRα). CD spectra were analyzed using CONTIN program and the SDP42 (185-240nm) database of CD Pro software [58]. As a negative control, CD spectra of 0.40μM of hGR (glucocorticoid receptor purchased from ThermoScientific), 0.44μM of hPPARα, and 0.2μM of hGR + 0.22μM of hPPARα were obtained and compared to the average spectrum of hGR and hPPARα. The CD spectrum of a mixture of each combination of proteins was compared to the calculated average of the individual proteins' spectra in order to determine whether structural changes occurred, suggesting a direct interaction between the proteins.

Protein-Protein Binding Assays/ Ligand Binding Assay

Binding assays of hPPARα and hLXRα were conducted using a PC1 fluorometer (ISS, Champaign, IL) to determine the binding affinities between the hPPARα and hLXRα. In order to obtain binding affinities (in terms of K_d), recombinant hPPARα was fluorescently labeled with a commercially available Cy5 Maleimide mono-reactive dye kit (Amersham, Pittsburgh, PA) that labels sulfhydryl groups, such as those on cysteine molecules present in the protein molecule. For optimum labeling, 1mg of hPPARα in buffer (Table 1) with a pH8.0 was incubated with Cy5 dye for 1 hour on a rotor and 30 minutes on the bench top at room temperature. The labeled protein was then separated from free dye by size exclusion chromatography in PBS, pH 7.4, and the molar concentration of the protein was estimated by Bradford assay, and the dye concentration

was measured by spectrophotometry using the molar extinction coefficient of the dye at 650nm. The dye to protein ratio determined using the molar concentrations of the protein and the dye resulted in 3 dyes labeled per protein molecule. Labeled hPPARα was titrated against an increasing concentration of unlabeled recombinant hLXRα, and was initially blanked using PBS. During the titration, between each addition, a 3min stir time was given for proper mixing and to allow equilibrium to be reached. 25nM Cy5-hPPARα, excited at 650nm was titrated against 0nM-250nM range of hLXRα, and the emission scanned from 660nm to 700nm yielded a peak around 670nm corresponding to the fluorescence emission, which was further used to calculate the binding affinity. Binding curves were then generated by non-linear regression analysis using the ligand binding function in Sigma Plot (SPSS, Chicago, IL). A double reciprocal plot was generated as previously described to determine the number of binding sites on the protein molecule [39]. In order to confirm that the binding of the two proteins was not just an artifact and not the effect of Cy5 dye, hLXRα was labeled with Cy3 dye and titrated against unlabeled hPPARα**.** The binding affinity of Cy3 labeled hLXRα with a dye to protein ratio of 2:1 was titrated against 0nM to 250nM of unlabeled hGR.

The binding affinity between hPPARα and hLXRα was also determined in the presence of the four LCFA and LCFA-CoA (mentioned in the CD experiments). In order to find the K_d, 25nM of both Cy5- hPPARα and the ligands were first mixed and then titrated against an increasing concentration of hLXRα (0nM to 250nM). Binding affinity of hPPARα and hLXRα were then determined in a similar way as described above.

TABLE 1. Composition of dialysis buffer

CHEMICAL NAME	CONCENTRATION
HEPES buffer	10mM
EDTA	0.1nM
DTT	0.4mM
KCl	100mM
Glycerol	10%

Co-Immunoprecipitation

Liver samples were extracted from 8-10 week old male C57BL/6J mice obtained from Jackson Laboratory. Mice were euthanized by CO_2 asphyxiation, and cervical dislocation was performed to ensure death per Wright State University LACUC approved protocols. Liver samples were extracted, chopped with a razor blade into fine pieces in 4mls of PBS, pH 7.4 and homogenized by sonication. The homogenate was then centrifuged at 10,000 rpm at 37^{o}C for 5 minutes (Eppendorf Centrifuge 5424). Pierce CoIP kit (ThermoScientific – 26149) was used to perform immuno-precipitation reactions per manufacturer's recommendations. This kit covalently links the antibodies to the resin, thereby preventing antibodies from being observed in the elutes. Total proteins from liver homogenates were quantified by Bradford assay and 400ul of liver sample containing 4mgs of total protein was incubated for 2 hours at room temperature with

resins coupled with PPARα and LXRα antibodies. A resin with no antibodies coupled to it was also used as a control. The resin was washed with wash buffer containing 1M NaCl and eluted using elution buffer provided in the kit. The elutions of about 50µl obtained from each resin was mixed with loading dye (0.3M Tris.HCl, 5% SDS and 50% glycerol), loaded on to a 12% SDS-PAGE gel for protein separation, and transferred to nitrocellulose membrane by electroblotting method for Western blot analysis. Blots were treated as explained above with anti-mouse monoclonal PPARα (ThermoScientific MA1-822) and anti-rabbit polyclonal LXRα (ThermoScientific: PA1-330).

Transactivation Assay

HepG2 cells (ATCC) that were 85-90% confluent were seeded onto four 24-well culture plates and grown overnight at 37^{o}C in a humidified CO_2 incubator as previously described [5]. The media in each well was replaced by 1ml of low-serum Eagles Minimum Essential Media (EMEM), and transfected with 0.4µg of respective plasmids. For overexpression of hPPARα and hLXRα in mammalian cells, pSG5 (Stratagene, La Jolla, CA), a eukaryotic expression vector containing an SV40 early promoter and polyadenylation signal that promotes expression in cells, was utilized. The DNA sequences encoding full length hPPARα and hLXRα were amplified from the bacterial expression vectors (described in protein expression in bacteria section) by PCR using the following the primers: CATCGGA TCCACC ATG GTG GAC ACG GAA AGC CCA and CCG GGA GCT GCA TGT GTC AGA GG (hPPARα), CATCGGA TCCACC ATG

TCC TTG TGG CTG GGG GCC CCT GTG and CCG GGA GCT GCA TGT GTC AGA GG (hLXRα). While a Bam HI / end-filled Sal I fragment was subsequently transferred into the multiple cloning site of pSG5 (Bam HI / end-filled Bgl II) to produce pSG5-hPPARα plasmid, Bam HI / end-filled Xho I fragment was subsequently transferred into the multiple cloning site of pSG5 (Bam HI / end-filled Bgl II) to produce pSG5-hLXRα. These plasmids encoding hPPARα, hLXRα and/or the empty vector pSG5 were transfected into the HepG2 cells with Lipofecatmine™ 2000 (Invitrogen) in accordance with the manufacturer's instructions. Each of the four plates was transfected with: (i) pSG5-hPPARα, (ii) pSG5-hLXRα, (iii) a mixture of pSG5-hPPARα and pSG5-hLXRα, or (iv) the empty pSG5 plasmid as a control. All four sets were also transfected with 0.4μg of a basic luciferase reporter construct (pGL4.17, Promega, Madison, WI) containing 2.3kb of the *ACOX* promoter upstream of the firefly luciferase gene. This plasmid was generated by amplifying the ACOX promoter region with the following primers ATGACTCTGTTTTCTATGACCT and GCTCCGAAGGTCAAGAAACT, and subsequently cloned into the pGL4.17 vector in the Hostetler laboratory by Mr. Dhawal Oswal. *ACOX* is a gene known to be regulated by PPARα and if upregulated would result in high luciferase activity indicating a positive regulation, and conversely, a decreased luciferase expression corresponding to reduced ACOX expression. In addition to this, all four sets were also transfected with 0.04ug of pRL-CMV plasmid (a eukaryotic expression vector for Renilla luciferase driven by the constitutive cytomegalovirus promoter CMV) as an internal control for transfection efficiency. Following transfection, cells were incubated for 6-8 hours at 37^{o}C in a humidified CO_2 incubator and then the

media were replaced by serum-free EMEM media for 1 hour to allow excess fatty acids to be utilized. The fatty acids were linked to BSA in order to facilitate their intake into the cells as previously described [59]. Four concentrations (1µM, 5µM, 10µM and 20µM) of these BSA-linked ligands (palmitic acid, oleic acid, linoleic acid and EPA) were added to the cells and the cells were grown for 20 additional hours to examine the effects of ligands on the activity of PPARα, LXRα and a mixture of the two proteins. Similar concentrations of the known PPARα activator, clofibrate (Sigma Aldrich 197777), were also used as a positive control [60]. The activity of firefly luciferase, normalized to Renilla luciferase that accounts for transfection efficiency, was determined using the dual-luciferase reporter assay kit (Promega,Madison, WI) and the sample with 1µM clofibrate was arbitrarily set to 100%. The luminescence was measured using a 96-well Microlite flat bottom microtitre plate (Thermo) using the SAFIRE^2 TECAN (Tecan Systems, Inc, San Jose, CA) for measuring luminescence.

Similar experiments were also conducted with a pGL4.17 plasmid encoding the SREBP-1c promoter, which was generated by amplifying the SREBP-1c promoter region with the following primers CGGTACCTCGAGCACTTGCAGGCTGGA and CGAGCTCGCCCCTAGGGCGTGCAGACG, and subsequently transferred into the Kpn I / Sac I sites of pGL4.17 in the Hostetler laboratory by Dr. S. Dean Rider, Jr. SREBP, known to be regulated by LXR was also examined to determine the effects of ligands on the activity of PPARα, LXRα and also a combination of the two proteins. The values for

SREBP were normalized and compared with the positive control (ACOX-Clofibrate) that was arbitrarily set to a 100%.

IV. RESULTS

SDS-PAGE and Western analysis showed the presence of a 50kDa protein that corresponded to the size of full length hPPARα and hLXRα

The full length recombinant proteins - hPPARα and hLXRα, purified using affinity chromatography, were run separately on 12% SDS-PAGE. The gels showed a band at around 50kDa, corresponding to the size of hPPARα (Figure 2A) and hLXRα (Figure 3A), which have a molecular weight of 52636Da and 51768Da respectively. Further, western blot analyses using antibodies for PPARα (Figure 2B) and LXRα (Figure 3B) confirmed the identity of the 52kDa band, further indicating the purification of full length, untagged protein. While the hPPARα gel shows a clear band at 52kDa and few lighter bands below, the corresponding Western also shows similar bands, suggesting that the other bands could be the degraded protein or a portion of hPPARα that was not completely translated. Similarly, the hLXRα gel as well as the Western shows a clear band at 50kDa and a few higher bands, which can be the LXR-LXR heterodimer.

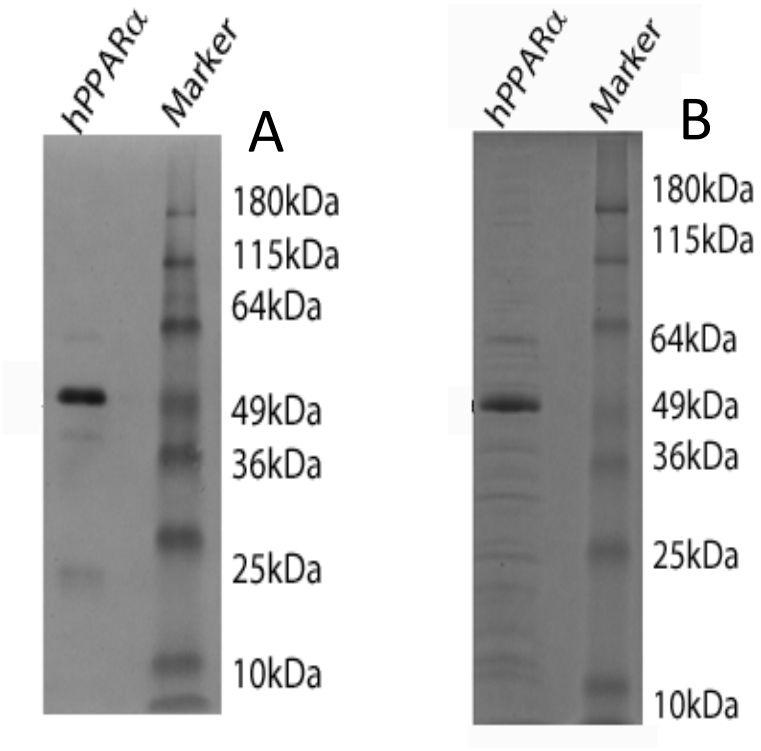

FIGURE 2: SDS-PAGE and a Western Blot showing full length hPPARα: (A) 12% SDS gel showing the 52kDa full length recombinant hPPARα protein purified by affinity chromatography using a GST affinity column. The gel was stained using Coomassie blue stain and destained in 7.5% acetic acid. **(B)** A western blot showing the 52kDa hPPARα band developed using an anti-mouse monoclonal antibody specific for the alpha isoform.

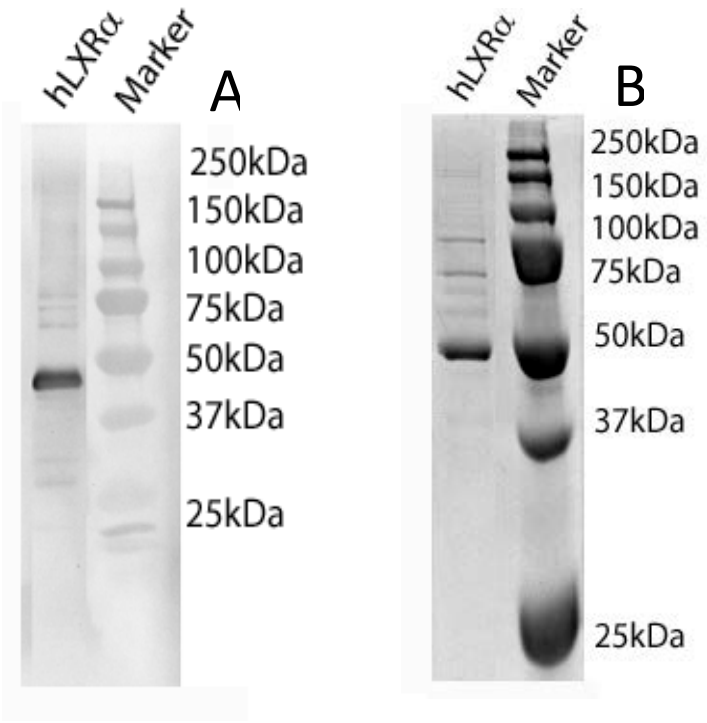

FIGURE 3: SDS-PAGE and a Western Blot showing full length hLXRα: (A) 12% SDS gel showing the 52kDa full length recombinant hLXRα protein purified by affinity chromatography using a GST affinity column, M – benchmark prestained marker (Invitrogen). The gel was stained using Coomassie blue stain and destained in 7.5% acetic acid. **(B)** A western blot showing the 52kDa hLXRα band developed using an anti-rabbit monoclonal antibody specific for the alpha isoform.

Circular Dichroism of hPPARα and hLXRα demonstrated conformational changes and suggested possible interaction between the two proteins

Circular dichroism, a spectrophotometric method used to determine the secondary structure of proteins, uses the principle of differential absorption of left and right circularly polarized light. This method was used to examine the secondary structure of full-length hPPARα and hLXRα individually and also as a mixture. While the CD spectra of hPPARα was characterized by a positive peak at approximately 190nm and two distinct negative peaks at 210nm and 220nm, the structure of hLXRα had a positive peak at 190nm and two small negative peaks at 210nm and 220nm (Figure 4); suggesting that LXRα has a less alpha helical structure. This was confirmed by examining the percent composition of each protein, which showed that each protein was also comprised of a considerable percentage of turns and unordered structures (Table 2). Although hPPARα and hLXRα displayed slightly different spectra, these data suggested that both proteins have structure and that the purification process did not denature the proteins.

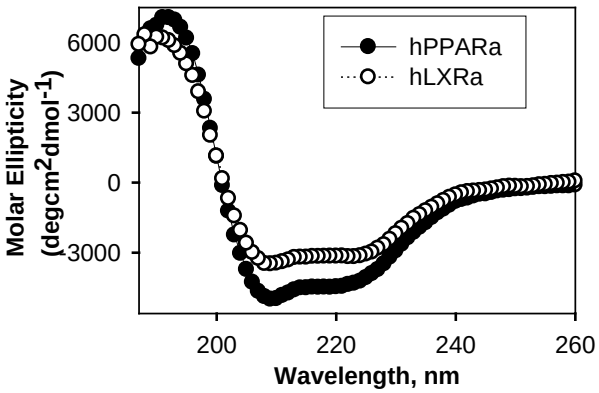

FIGURE 4: Circular dichroic spectra of hPPARα and hLXRα. Circular dichroic spectra of 0.42μM hPPARα alone (closed circle), showing a positive peak at 190nm and two negative peaks at 210nm and 220nm and 0.44μM hLXRα alone (open circle) showing one positive peak at around 190nm and two small negative peaks at 210nm and 220nm.

TABLE 2. Secondary structure of hPPARα and hLXRα in the absence of ligands

Protein	α-helix regular H(r) %	α-helix distorted H (d) %	β-sheet regular S(r) %	β-sheet distorted S (d) %	Turns T%	Unrd U%
PPARα	7.2 ± 2.6	7.8 ± 0.9	21.2 ± 2	10.2 ± 1.1	17.7 ± 2	36.4 ± 3.5
LXRα	5.8 ± 2.4	5.7 ± 0.6	20.4 ± 3.2	9.3 ± 1.5	15.6 ± 3.4	43.1 ± 5
GR	0.7 ± 0.1	3.9 ± 0.2	24 ± 0.3	12 ± 0.7	19.6 ± 2	39.3 ± 2.7
PPARα+LXRα (Exp)	5 ± 1.5	6.2 ± 1.4	17.3 ± 3	10.8 ± 3	23.4 ± 7	37 ± 6.2
PPARα+LXRα (CA)	5.4 ± 1.7	6.3 ± 0.5	21.2 ± 2.3	9.2 ± 1.3	16 ± 2.8	41.4 ± 4.4
PPARα+GR (Exp)	7.2 ± 1.8	7.1 ± 0.3	19.5 ± 2.2	8.2 ± 1.8	14 ± 4.2	43.8 ± 6.7
PPARα+GR (CA)	4.5 ± 2.8	6 ± 0.4	19 ± 2.8	9 ± 2.4	14.6 ± 5	45.2 ± 7.4

PPARα, peroxisome proliferator activated receptor-α; LXRα, Liver x receptor-α, GR, glucocorticoid receptor; Unrd, unordered

Exp – experimental, CA – Calculated average

Furthermore, a mixture of hPPARα and hLXRα at equal amino acid molar concentrations underwent a change in conformation, and assumed a structure close to that of an alpha helix structure, however displaying one positive peak at 190nm and one distinctive negative peak at around 210nm, with a smaller peak at 220nm (Figure 5A). The change in the structure of the proteins can determine the possibility of either an interaction or no interaction, which is interpreted by comparing the actual (or experimental) spectra with the calculated average obtained by averaging the individual spectrum of the two proteins. While a spectrum overlaying the calculated average suggests no interaction between the two proteins, a spectrum that is different from the calculated average suggests a possible interaction. In this experiment the actual spectrum was slightly different from the calculated average, suggesting the probability of an interaction between the proteins. Further, when equal concentrations of hPPARα and hGR were run as a control, the spectra representing the actual change overlapped the calculated average of the two spectra (Figure 5B) suggesting no interaction between the two proteins. This was further substantiated by comparing the lack of significant differences in the percent compositions (Table 2).

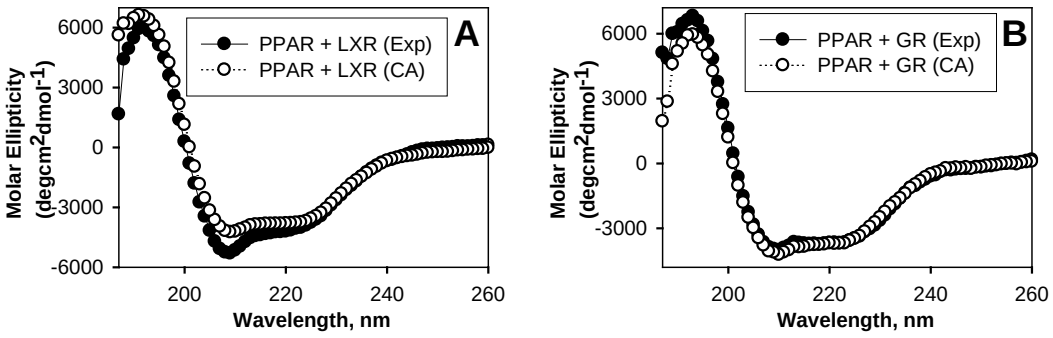

FIGURE 5: Circular dichroic spectra of a combination of two proteins. **(A)** Circular dichroic spectra of hPPARα and hLXRα demonstrated a change in the secondary structure. Circular dichroic spectra of a mixture of 0.21μM hPPARα and 0.22μM hLXRα (closed circle) and an average of hPPARα and hLXRα spectra (open circle) representing no interaction between the two proteins. **(B)** Negative control showing no interaction between hPPARα and hGR where the actual spectrum of hPPARα and GR (open circle) superimposes on the average of the hPPARα and hGR spectrum (closed circle).
Exp – experimentally obtained spectra, CA – calculated average.

Circular Dichroism of hPPARα and hLXRα in the presence of fatty acids and their CoA

Circular dichroic spectra of the mixture of hPPARα and hLXRα were obtained in the presence of fatty acids and their CoA thioesters to examine their effects on hPPARα and hLXRα's structural conformation and interaction. Conformational changes of proteins are very significant as they determine the function of the protein, and any change in conformation may result in folding of a protein in such a way that it can either promote or inhibit it's interaction with other proteins, ligands, or DNA. In order to determine the effect of fatty acids or their CoA thioesters, several spectra were obtained. First, the

experimental CD spectrum of each protein was obtained individually in the presence and absence of each fatty acid or fatty acyl-CoA. Next, the experimental CD spectrum of a mixture of equal molar concentrations of hPPARα and hLXRα was obtained in the presence of each fatty acid or fatty acyl-CoA. Then the actual spectra obtained for a mixture of hPPARα and hLXRα in the presence of fatty acids or fatty acyl-CoA was compared to (i) the spectra of hPPARα and hLXRα in the absence of ligand, (ii) the calculated average of each protein in the presence of that particular ligand, (iii) the calculated average of hPPARα bound to ligand and hLXRα, (iv) the calculated average of hLXRα bound to ligand and hPPARα (Table 4 and Table 5). An experimentally obtained spectrum similar to the one obtained from hPPARα and hLXRα in the absence of ligand would suggest that the ligand had no effect on the interaction between the two proteins (Figure 6A). However, a spectrum similar to the calculated average of hPPARα and hLXRα the presence of ligand would suggest the inhibition of protein interaction due to the ligand (Figure 6B). Further, spectra resembling the calculated average of hPPARα in the presence of ligand and hLXRα in the absence of ligand or hLXRα in the presence of ligand and hPPARα in the absence of ligand would suggest that the binding of the ligand to either of the proteins inhibits the protein-protein interaction. However, a spectrum dissimilar to each of these comparisons would suggest a new conformation, most likely of all three components (hLXRα, hPPARα, and ligand).

Circular dichroic spectra of hPPARα and hLXRα with a saturated fatty acid - palmitic acid (Figure 6A), were superimposable on the spectra of a mixture of hPPARα

and hLXRα in the absence of fatty acid, suggesting no conformational change and therefore proposing no effect of palmitic acid on the protein-protein interaction. However, its thioester form; palmitoyl-CoA (Figure 6B) displayed a significant change in conformation and lay on the average of the two spectra suggesting that the CoA thioester might interfere with the interaction between hPPARα and hLXRα and could potentially decrease the binding affinity.

Oleic acid (Figure 6C) displayed a similar trend to that of palmitoyl-CoA by being superimposable on the spectrum of the average of hPPARα and hLXRα suggesting a decreased interaction between the two proteins, while its CoA thioester (Figure 6D) showed a very small structural change indicating an effect of oleoyl-CoA on the interaction between the two proteins.

In the case of linoleic acid (Figure 7A) and eicosapentaenoic acid (EPA) (Figure 7C), two polyunsaturated fatty acids, both displayed a similar trend, where the average spectra almost overlaid on the mixture of the two proteins with ligand suggesting that linoleic acid and EPA possibly interfered with the interaction between the two proteins. Conformational changes observed with the CoA derivatives of both fatty acids - linoleoyl CoA (Figure 7B) and EPA-CoA (Figure 7D) were similar to one another suggesting that they could also interfere with hPPARα and hLXRα to prevent the two proteins from interacting.

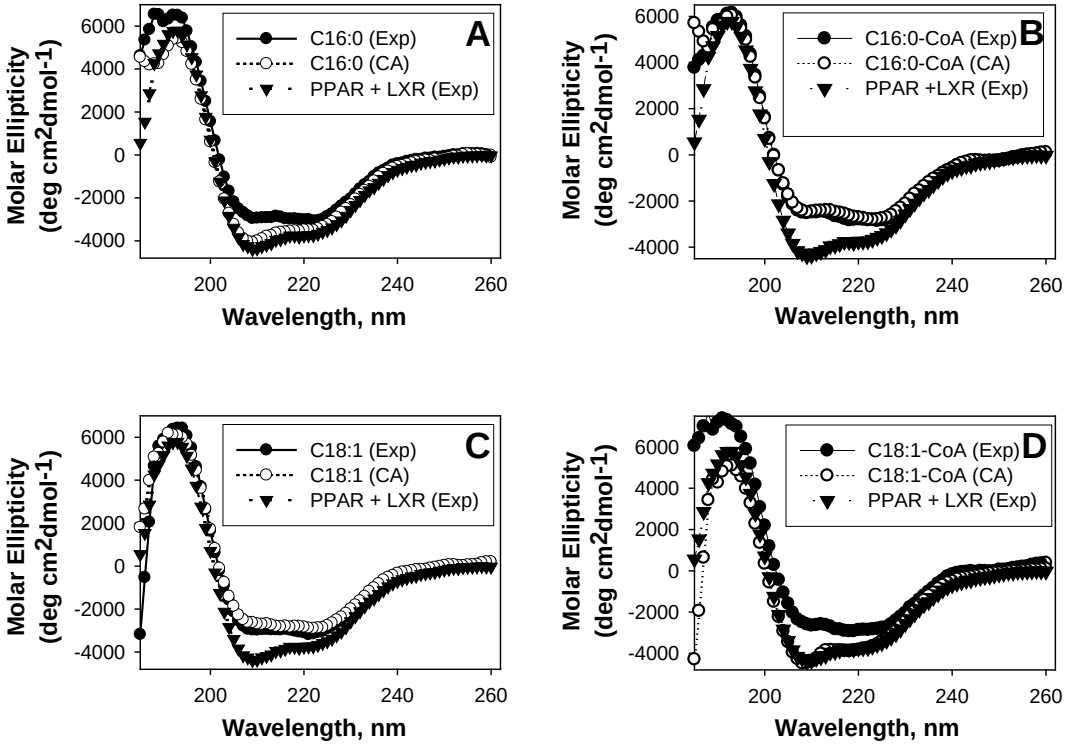

FIGURE 6: CD spectra of a mixture of hPPARα and hLXRα in the presence and absence of fatty acids and their CoA thioesters. Far-UV spectra of a mixture of equal amino acid molarities of hPPARα and hLXRα in the absence of ligands (closed inverted triangles), a mixture of equal amino acid molarities of hPPARα and hLXRα in presence of ligand (closed circles), and the theoretically expected spectrum of the two proteins in the presence of ligand if no interaction occurred between hPPARα and hLXRα, obtained by averaging the spectrum of hPPARα plus ligand with the spectrum of hLXRα plus ligand (open circles). Ligands include: **(A)** C16:0, **(B)** C16:0-CoA, **(C)** C18:1, and **(D)** C18:1-CoA. Each spectrum is a representative of an average of ten scans and is taken from three replicates.

Exp – experimentally obtained spectra, CA – calculated average.

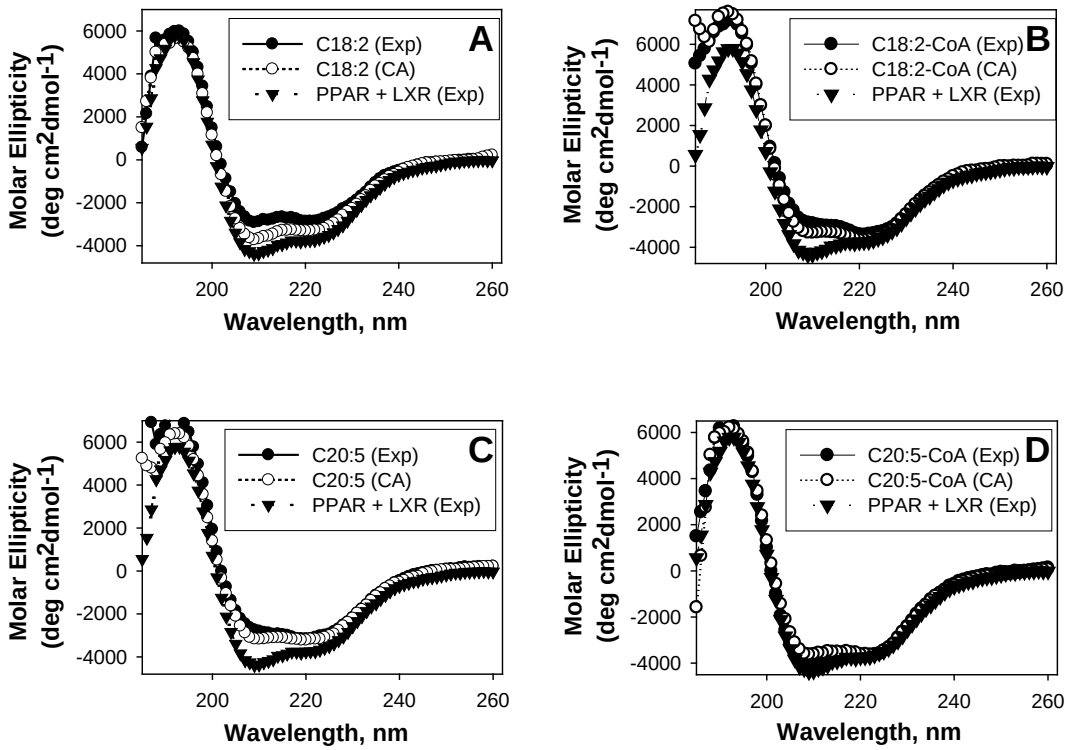

FIGURE 7: CD spectra of a mixture of hPPARα and hLXRα in the presence and absence of fatty acids and their CoA thioesters. Far-UV spectra of a mixture of equal amino acid molarities of hPPARα and hLXRα in the absence of ligands (closed inverted triangles), a mixture of equal amino acid molarities of hPPARα and hLXRα in presence of ligand (closed circles), and the theoretically expected spectrum of the two proteins in the presence of ligand if no interaction occurred between hPPARα and hLXRα, obtained by averaging the spectrum of hPPARα plus ligand with the spectrum of hLXRα plus ligand (open circles). Ligands include: **(A)** C18:2, **(B)** C18:2-CoA, **(C)** C20:5, and **(D)** C20:5-CoA. Each spectrum is a representative of an average of ten scans and is taken from three replicates.

Exp – experimentally obtained spectra, CA – calculated average.

TABLE 3. Secondary structures of hPPARα and hLXRα (corrected for solvent effect) in the presence of fatty acids and their CoA thioesters

Protein	α-helix regular	α-helix distorted	β-sheet regular	β-sheet distorted	Turns	Unrd
	H(r) %	H (d) %	S(r) %	S (d) %	T%	U%
PPARα + solvent	5.1 ± 1.6	6.5 ± 0.3	22.3 ± 2.3	9.8 ± 0.7	17.9 ± 0.9	38.3 ± 1.9
PPARα + C16:0	6.6 ± 5.1	6.5 ± 1.4	19.9 ± 6.0	7.5 ± 3.1	11.9 ± 6.1	47.6 ± 8.4
PPARα + C16:0 -CoA	1.5 ± 0.6	5.4 ± 0.3	26.3 ± 1.4	10.6 ± 0.4	18.6 ± 1.3	37.6 ± 1.3
PPARα + C18:1	6.0 ± 3.9	5.9 ± 0.6	20.8 ± 4.4	7.6 ± 2.8	12.3 ± 6.2	47.4 ± 8.9
PPARα + C18:1-CoA	4.8 ± 1.7	6.6 ± 0.9	22.8 ± 1.5	11 ± 0.6	20.2 ± 0.6	34.5 ± 2
PPARα + C18:2	3.4 ± 1.5	6.3 ± 0.8	23.5 ± 1.4**	10.5 ± 0.9	19.6 ± 1.7	36.8 ± 2.7
PPARα + C18:2-CoA	3.8 ± 1.6	6.5 ± 0.8	24.1 ± 2.6	10.1 ± 0.8	18.1 ± 0.4	37.4 ± 1.2
PPARα + C20:5	5.8 ± 4.2	6.1 ± 0.9	21.1 ± 5.5	8 ± 2.9	12.4 ± 6.2	46.7 ± 9.5
PPARα + C20:5-CoA	5.6 ± 3.3	23.4 ± 14.9	19.2 ± 4.2	8.1 ± 3.5	15.9 ± 5.1	43.7 ± 7.5
LXRα + solvent	4 ± 1.5	6.1 ± 0.7	21.4 ± 2	10.3 ± 2.1	18.1 ± 2.5	39.7 ± 4.5
LXRα + C16:0	3.6 ± 4.3	5.4 ± 0.9	21.8 ± 6.8	57.5 ± 29.8	15.7 ± 6	44.3 ± 11.1
LXRα + C16:0 -CoA	8.5 ± 3.1	7.3 ± 1.1	13 ± 4.4	4.3 ± 4.3	7.2 ± 7.2	59.2 ± 12
LXRα + C18:1	1 ± 0.4	4.3 ± 0.4	25.1 ± 1.9	12.9 ± 2.0	22.5 ± 3.9	34.3 ± 3.9
LXRα + C18:1 -CoA	1 ± 0.3	15.7 ± 10.6	22.6 ± 1.9	15.1 ± 0.5	23.4 ± 1.9	33.2 ± 2.1
LXRα + C18:2	3 ± 0.4	7.2 ± 0.4	24.3 ± 0.9	9.8 ±0.6	19.7 ± 1.2	36.1 ± 1.3
LXRα + C18:2 -CoA	4.8 ± 2.5	7.1 ± 1.5	20.4 ± 4.5	7.4 ± 3.2	16.2 ± 3	44.1 ± 6.7
LXRα + C20:5	5.2 ± 2.7	6 ± 1.1	19.3 ± 3.9	8.6 ± 4.4	15.1 ± 6.2	45.9 ± 10.6
LXRα + C20:5 -CoA	7.5 ± 7.1	5.5 ± 1.8	16.1 ± 8.8	5.8 ± 2.5	10 ± 6.8	55.3 ± 15.7

Asterisks (*) represent significant differences due to presence of ligand as compared with the no-ligand for all the panels. *$p < 0.05$, **$p < 0.01$, ***$p < 0.001$.

TABLE 4. Secondary structures of hPPARα and hLXRα, individually and as a mixture (corrected for solvent effect) in the presence and absence of fatty acids

Protein	α-helix regular	α-helix distorted	β-sheet regular	β-sheet distorted	Turns	Unrd
	H(r) %	H (d) %	S(r) %	S (d) %	T%	U%
PPARα+LXRα+solvent	4.2 ± 2.9	5.3 ± 2.9	14.5 ± 6.1	11.5 ± 6	28 ± 14.6	36.3 ± 11.9
PPARα+16:0 and LXRα (CA)	3.8 ± 1.7	6.4 ± 0.8	23.8 ± 2.4	9.7 ± 0.1	18 ± 1.1	38.1 ± 1.5
LXRα+16:0 and PPARα (CA)	8 ± 3.7	6.5 ± 0.9	16 ± 6	11.8 ± 2.3	17 ± 51.8	51.8 ± 11
PPARα+LXRα+16:0 (Exp)	3.7 ± 3	5.5 ± 1	21.4 ± 3.8	9.8 ± 1.9	17.1 ± 2.8	40.8 ± 5.2
PPARα+16:0 and LXRα+16:0 (CA)	4.3 ± 1.7	6.2 ± 0.6	22.3 ± 2	9.4 ± 1.8	16 ± 3	41.6 ± 5
PPARα+18:1 and LXRα (CA)	4.8 ± 3.4	6.3 ± 0.5	22.6 ± 4.5	8.53 ± 2.7	14.2 ± 5.2	43.4 ± 8.5
LXRα+18:1 and PPARα (CA)	1.3 ± 0.5	4.5 ± 0.4	25 ± 0.5	13 ± 1.5	22.7 ± 3	33.4 ± 4
PPARα+LXRα+18:1 (Exp)	1.4 ± 0.6	4.8 ± 0.4	23.7 ± 0.3	13.6 ± 1.4	24.1 ± 2.7	32.1 ± 3
PPARα+18:1 and LXRα+18:1 (CA)	1.3 ± 0.5	5 ± 0.3	26 ± 1	11.7 ± 1.4	19.7 ± 2.1	36.2 ± 2.2
PPARα+18:2 and LXRα (CA)	3.5 ± 18	6.3 ± 0.4	23.7 ± 1.7	10 ± 1.3	18 ± 2.5	38.4 ± 3.4
LXRα+18:2 and PPARα (CA)	1.7 ± 0.7	5 ± 0.4	25.1 ± 0.6	12 ± 0.8	20.7 ± 0.9	35.5 ± 1.4
PPARα+LXRα+18:2 (Exp)	1 ± 0.4	4.8 ± 0.2	26 ± 1.4	12 ± 1.2	20.3 ± 2.2	35.8 ± 2
PPARα+18:2 and LXRα+18:2 (CA)	1.7 ± 0.1	5.3 ± 0.1	25.4 ± 0.5	11.4 ± 0.3	20.1 ± 0.8	36 ± 1.3
PPARα+20:5 and LXRα (CA)	5.3 ± 3.5	6 ± 0.4	21.9 ± 4.6	8.3 ± 2.7	13 ± 6.2	44.7 ± 9.5
LXRα+20:5 and PPARα (CA)	1.7 ± 0.6	5.5 ± 0.2	26.3 ± 3.1	11 ± 1.2	18.8 ± 2.6	36.5 ± 1.2
PPARα+LXRα+20:5 (Exp)	8.4 ± 3.8	6.2 ± 0.4	18.8 ± 5.3	5 ± 2.2	10.6 ± 4.8	56 ± 8.2
PPARα+20:5 and LXRα+20:5 (CA)	5.4 ± 3	6 ± 0.2	20.7 ± 3.8	14.4 ± 2.8	19.8 ± 0.4	46 ± 10.4

Exp – Experimental, CA – Calculated Average

TABLE 5. Secondary structures of hPPARα and hLXRα, individually and as a mixture (corrected for solvent effect) in the presence and absence of fatty acyl CoAs

Protein	α-helix regular H(r) %	α-helix distorted H (d) %	β-sheet regular S(r) %	β-sheet distorted S (d) %	Turns T%	Unrd U%
PPARα+LXRα+solvent	4.2 ± 2.9	5.3 ± 2.9	14.5 ± 6.1	11.5 ± 6	28 ± 14.6	36.3 ± 11.9
PPARα+16:0-CoA and LXRα (CA)	5 ± 1.8	7 ± 0.7	21.4 ± 2.5	9.9 ± 1.1	18.7 ± 1.7	37.9 ± 3.1
LXRα+16:0-CoA and PPARα (CA)	8.9 ± 3.3	6.6 ± 0.5	15.8 ± 5.1	5.8 ± 3.3	13.7 ± 5.6	55.3 ± 11
PPARα+16:0-CoA and LXRα+16:0-CoA (CA)	5.8 ± 1.7	7.2 ± 0.9	20 ± 2.4	7.3 ± 2.7	10.5 ± 6	48.4 ± 7.4
PPARα+LXRα+16:0-CoA (Exp)	3.1 ± 2.3	5.5 ± 0.8	23.1 ± 3.4	9.8 ± 2	16.4 ± 3.1	41.9 ± 4.7
PPARα+18:1-CoA and LXRα (CA)	5.6 ± 2.1	7.7 ± 0.4	21.8 ± 3.1	10.4 ± 1.6	18.3 ± 3	35.7 ± 5.7
LXRα+18:1-CoA and PPARα (CA)	1.7 ± 0.3	5.3 ± 0.2	25.4 ± 1.6	13 ± 0.3	21 ± 0.2	33.4 ± 1.9
PPARα+18:1-CoA and LXRα+18:1-CoA (CA)	2.5 ± 0.5	5.7 ± 0.4	24.8 ± 0.6	13.3 ± 0.1	21.7 ± 0.5	31.87 ± 0.9
PPARα+LXRα+18:1-CoA (Exp)	4.9 ± 1.5	6.8 ± 0.9	21.3 ± 2.2	9.3 ± 2.3	17.9 ±3	39.5 ± 5.2
PPARα+18:2-CoA and LXRα (CA)	4.5 ± 2.1	7.2 ± 0.6	22.5 ± 3.5	9.7 ± 0.9	19.2 ± 1.6	36.7 ± 3.3
LXRα+18:2-CoA and PPARα (CA)	5.9 ± 3	6.2 ± 0.3	21 ± 3.9	8.5 ± 3.1	19.5 ± 0.4	45.3 ± 10
PPARα+18:2-CoA and LXRα+18:2-CoA (CA)	6.6 ± 2.7	7 ± 0.7	19.3 ± 3.3	7.9 ± 2.5	14.4 ± 4.9	44.5 ± 7.8
PPARα+LXRα+18:2-CoA (Exp)	5.2 ± 3.5	5.5 ± 1	20.2 ± 4.7	8.3 ± 4.4	12.9 ± 6.5	47.5 ± 10
PPARα+20:5-CoA and LXRα (CA)	5.1 ± 1.7	7.3 ± 0.2	21.6 ± 2.9	10.4 ± 1.7	18.9 ± 2.7	36.5 ± 5.4
LXRα+20:5-CoA and PPARα (CA)	6.2 ± 3.5	7.1 ± 0.8	18.5 ± 2.6	6 ± 1.9	11.1 ± 3.3	50.2 ± 4.5
PPARα+20:5-CoA and LXRα+20:5-CoA (CA)	7.5 ± 3.7	6.5 ± 1.1	16.5 ± 4.1	7.7 ± 4	11.6 ± 6	51.1 ± 8.7
PPARα+LXRα+20:5-CoA (Exp)	1.6 ± 0.4	4.7 ± 0.6	24.3 ± 0.5	12.6 ± 1.1	22.5 ± 1.5	34.1 ± 2.2

Exp – Experimental, CA – Calculated Average

Cy5-hPPARα and hLXRα interact with a strong binding affinity

As the CD spectrum only shows a change in conformation, and cannot completely determine if the conformational change is due to an efficient interaction with the other protein or ligand, binding assays were conducted with hPPARα and hLXRα in the presence and absence of ligands to determine the binding affinity.

While the CD spectra of the mixture of the hPPARα and hLXRα suggested a possible interaction, the direct binding assay of Cy5 labeled hPPARα and hLXRα further confirmed high affinity binding of the two proteins, with binding affinities in the nanomolar range. A titration of Cy5-hPPARα against an increasing concentration of hLXRα ranging from 0nM to 250nM resulted in strong saturable binding and very high affinity binding (K_d = 6±2nM, Figure 8C), and the double reciprocal plot (inset) further suggested a single binding site. In order to ensure that the two proteins directly interact and that the results obtained were not an artifact of the fluorophore added to the PPARα protein, Cy3 labeled hLXRα protein was also titrated with GR protein. While increasing concentrations of GR resulted in increased fluorescence intensity, the shape of the curve was non-saturable and almost linear (Figure 8B), suggesting only nonspecific binding (K_d > 270nM). To further ensure that the binding of hPPARα and hLXRα was due to true protein-protein interaction, Cy3 labeled hLXRα was titrated with increasing concentrations of hPPARα (Figure 8A). This titration resulted in strong saturable binding

(Figure 8C), although with slightly lower affinity (K_d = 42±16nM), further confirming the binding of hPPARα and hLXRα.

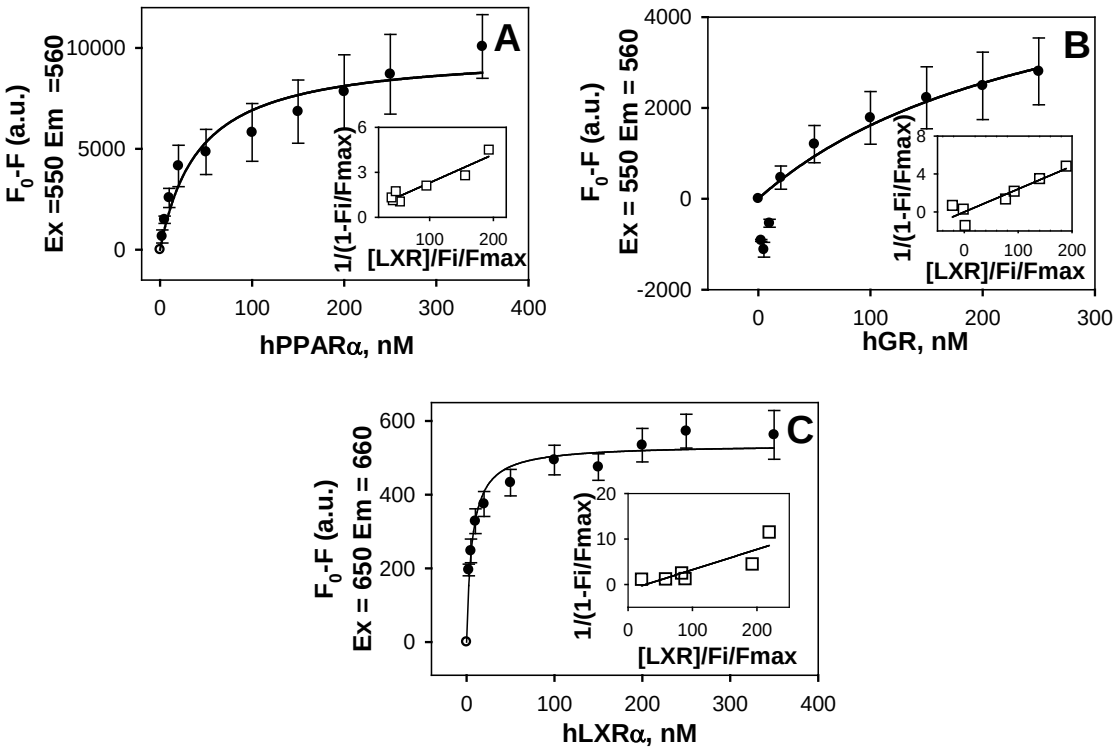

FIGURE 8: Fluorescent binding assays with labeled protein titrated against increasing concentrations of unlabeled protein. (A) 25nM of Cy3hLXRα was titrated against increasing concentrations of 0nM to 250nM hPPARα. The x-axis represents the concentration of hPPARα used and the y-axis represents the change in fluorescence intensity. **(B)** 25nM of Cy3hLXRα was titrated against increasing concentrations of 0nM to 250nM hGR. The x-axis represents the concentration of hGR used and the y-axis represents the change in fluorescence intensity. **(C)** 25nM of Cy5hPPARα was titrated against increasing concentrations of 0nM to 250nM hLXRα. The x-axis represents the concentration of hLXRα used and the y-axis represents the change in fluorescence intensity. Insets represent double reciprocal linear plots of each binding curve. Values represent mean ± SE; n = 3-6

hPPARα and hLXRα Binding in presence of Ligands

After confirming the direct binding of hPPARα and hLXRα with high affinity, the effects of fatty acids and their CoA thioesters such as palmitic acid, palmitoyl-CoA, oleic acid, oleoyl-CoA, linoleic acid, linoleoyl-CoA, EPA and EPA-CoA on the binding affinity were examined. While the saturated fatty acid – palmitic acid (Figure 9A) did not affect the interaction between Cy5hPPARα and hLXR and displayed a similar K_d of 7±2nM as that of the two proteins in the absence of a ligand (Figure 8C), its CoA thioester palmitoyl-CoA (Figure 9B) slightly decreased the binding affinity yielding a K_d of 53±17nM. On the other hand, the unsaturated fatty acid – oleic acid (Figure 9C) marginally decreased the binding of the two proteins with a K_d of 37±10nM, when compared to its CoA form- oleoyl-CoA (Figure 9D) that displayed a binding affinity of 27±12nM.

Further assays with polyunsaturated fatty acids, linoleic acid and EPA, showed decreased binding of Cy5hPPARα and hLXRα suggesting that the fatty acids may interact with one or both of the proteins causing a conformational change such that the binding ability is altered. While linoleic acid (Figure 10A) decreased the binding affinity, yielding an increased K_d of 151±93nM, EPA (Figure 10C) strongly decreased the binding and resulting in a K_d greater than 600nM. The CoA thioesters of the two fatty acids also decreased the binding affinity; while the K_d of 36±11nM displayed by linoleoyl CoA (Figure 10B) was much similar to that of oleic acid, EPA-CoA (Figure

10D) caused a large change in interaction between the proteins, and generated a K_d of 135±160nM suggesting an interference with the binding.

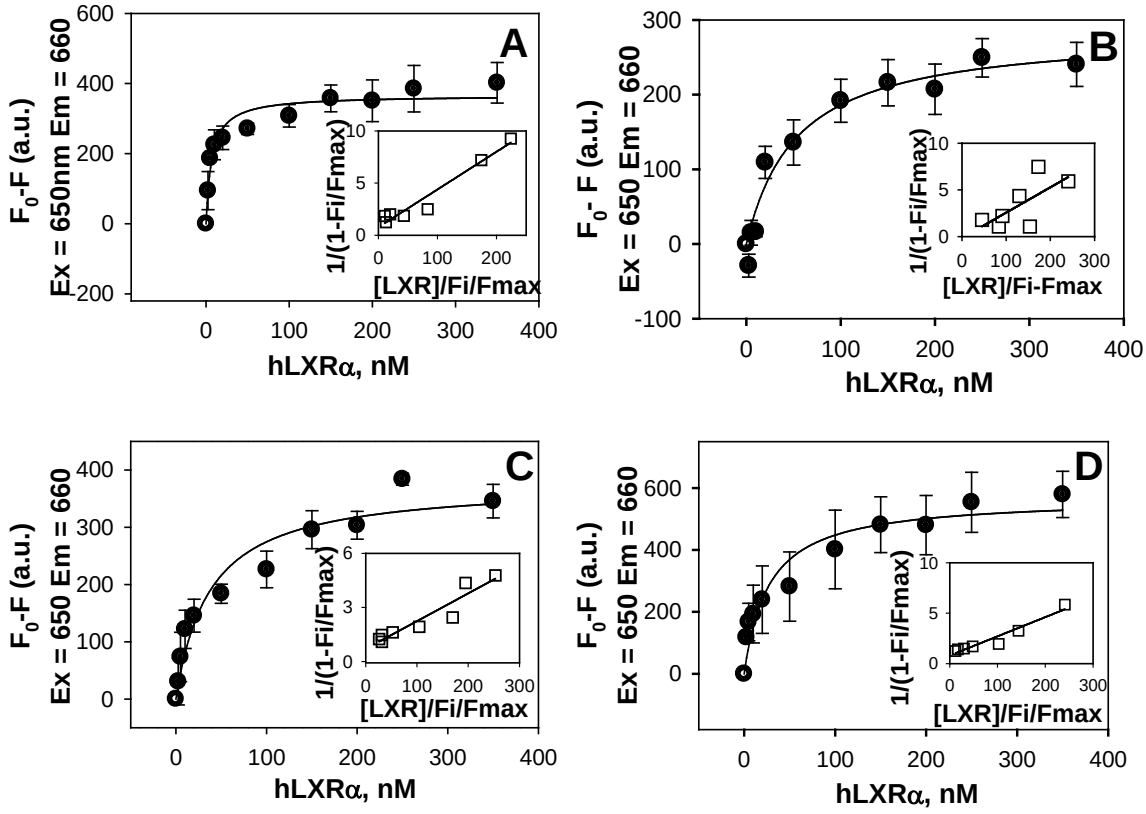

FIGURE 9: Binding curves of the change in fluorescent intensity (Fo-F) of a mixture of equal concentrations of the fluorescently labeled Cy5hPPARα and the ligand titrated with increasing concentrations of hLXRα. Binding curves of 25nM Cy5hPPARα titrated against hLXRα in the presence of 25nM of ligands **(A)** palmitic acid**, (B)** its CoA thioester – palmitoyl CoA, **(C)** Oleic acid and **(D)** Oleoyl-CoA

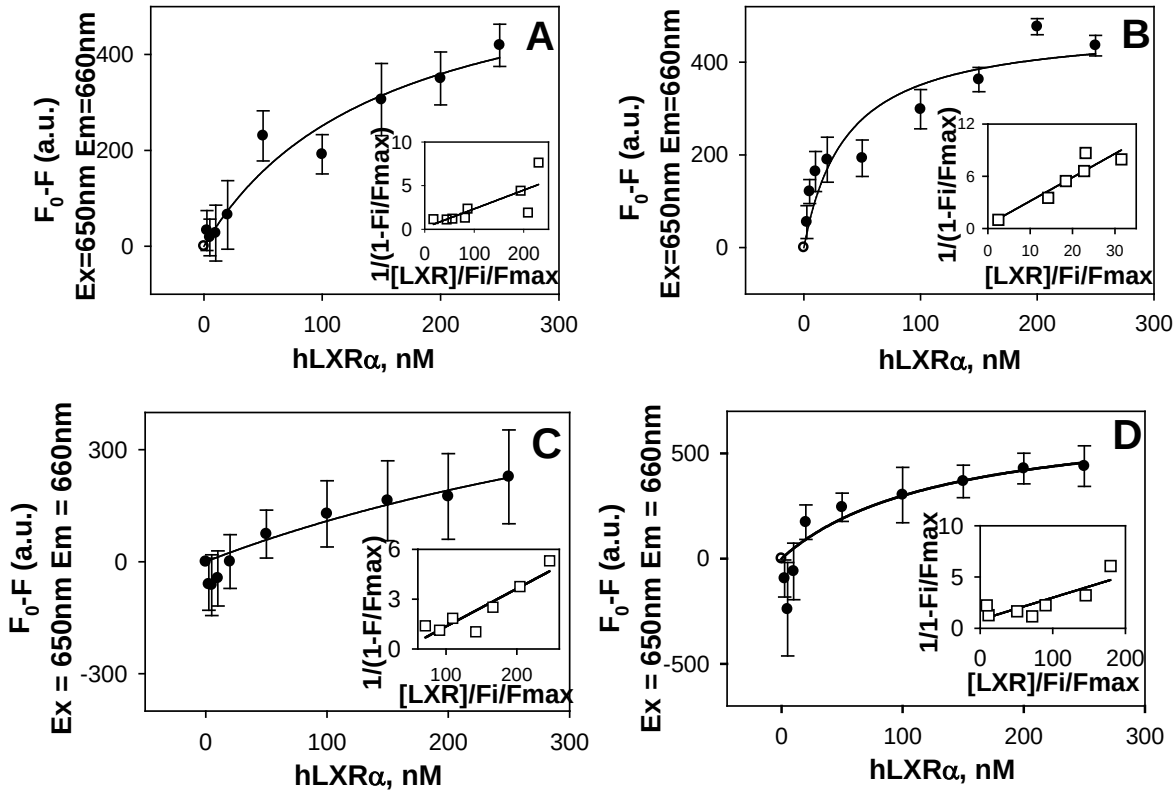

FIGURE 10: Binding curves of the change in fluorescent intensity (Fo-F) of a mixture of equal concentrations of the fluorescently labeled Cy5hPPARα and the ligand titrated with increasing concentrations of hLXRα. Binding curves of 25nM Cy5hPPARα titrated against hLXRα in the presence of 25nM of ligands **(A)** linoleic acid, **(B)** linoleoyl-CoA, **(C)** EPA and **(D)** EPA-CoA.

Co-Immunoprecipitation: PPARα and LXRα show direct interaction in mouse liver homogenates

After the interactions and binding of the two recombinant nuclear receptors, hPPARα and hLXRα, were observed *in vitro* with circular dichroism and binding assays, the interaction between PPARα and LXRα was tested *in vivo*. Co-immunoprecipitation of liver samples with PPARα or LXRα antibodies, and subsequent Western blot analysis for PPARα (Figure 10A) or LXRα (Figure 10B) protein, resulted in bands corresponding to 50kDa for liver homogenate and each antibody linked resin, further suggesting a direct interaction of PPARα and LXRα. The bands in both PPARα (Figure 11A) and LXRα (Figure 11B) Western blots show strong bands, however at a slightly higher molecular weight than 50kDa. This shift in the bands could be due to post-translational modifications of the proteins that occur endogenously. As a control, elute obtained from resin coupled with no antibodies was run along with the other samples in order to confirm that the binding of the proteins to their antibodies was not just an artifact. The lane with elute obtained from resin with no antibody did not show any bands, further confirming the antibody-specific binding of the proteins.

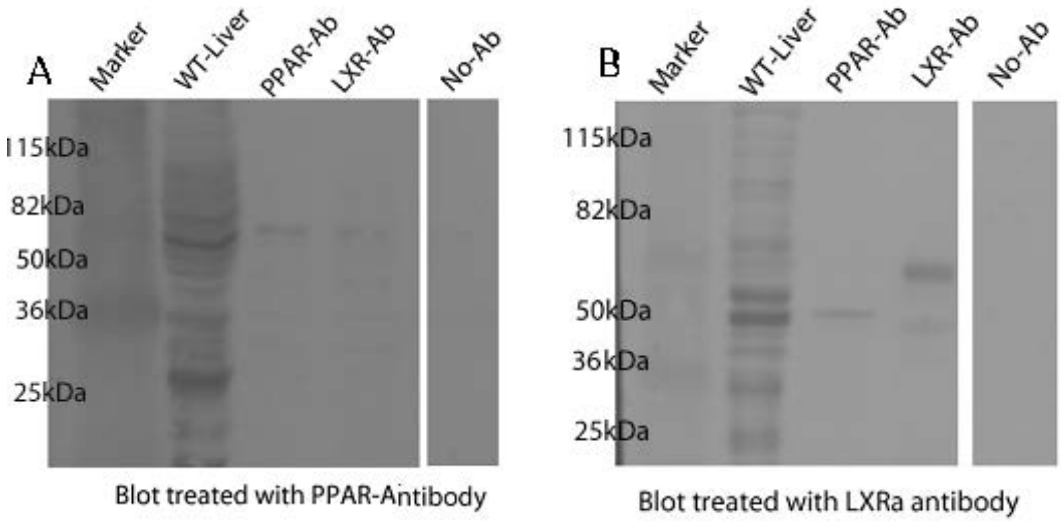

FIGURE 11: CoIP assay using wild type mouse liver sample showing interaction of PPAR and LXR. (A) Western of a mouse liver sample passed through resin coupled with PPARα- and LXRα-antibody and treated with PPARα antibody. **(B)** Western of a mouse liver sample passed through resin coupled with PPARα- and LXRα-antibody and treated with LXRα antibody.

Transactivation Assay

In order to determine the significance of these findings, the ability of the PPARα ligands palmitic acid, oleic acid, linoleic acid and EPA to affect either a PPARα regulated gene (acyl-CoA oxidase, ACOX) or an LXRα regulated gene (SREBP) was examined. ACOX is known to play a role in fatty acid metabolism, while SREBP regulates cholesterol metabolism [61]. Activity was measured with a reporter construct for luciferase expression, and the relative amount of luciferase produced in the presence of clofibrate, palmitic acid, oleic acid, linoleic acid and EPA was compared to the activity of the two proteins in the absence of ligands. Four concentrations (1μM, 5μM, 10μM and 20μM) of each ligand were tested for the effect on relative PPARα or LXRα activity.

The transactivation of the PPARα gene ACOX was fairly consistent throughout, both in the groups treated with no ligand as well as those treated with ligands. In all instances, the presence of both PPARα and LXRα (diamond bars) showed higher activity than either PPARα (open bars) or LXRα (forward hash bars) alone, although the extent of this affect was ligand dependent (Figure 12). This suggested that PPARα and LXRα heterodimerization could increase PPARα regulated transactivation. While lower concentrations of the ligands palmitic acid, oleic acid, linoleic acid and EPA (1μM, Figure 12A and 5μM, Figure 12B) did not seem to affect the expression of ACOX, the higher ranges (10μM, Figure 12C and 20μM, Figure 12D) of palmitic acid and oleic acid slightly increased the expression. Furthermore, cells treated with pSG5 (backward hash

bars) showed consistent luciferace expression, representing the effect of basal level expression of PPARα in HepG2 cells.

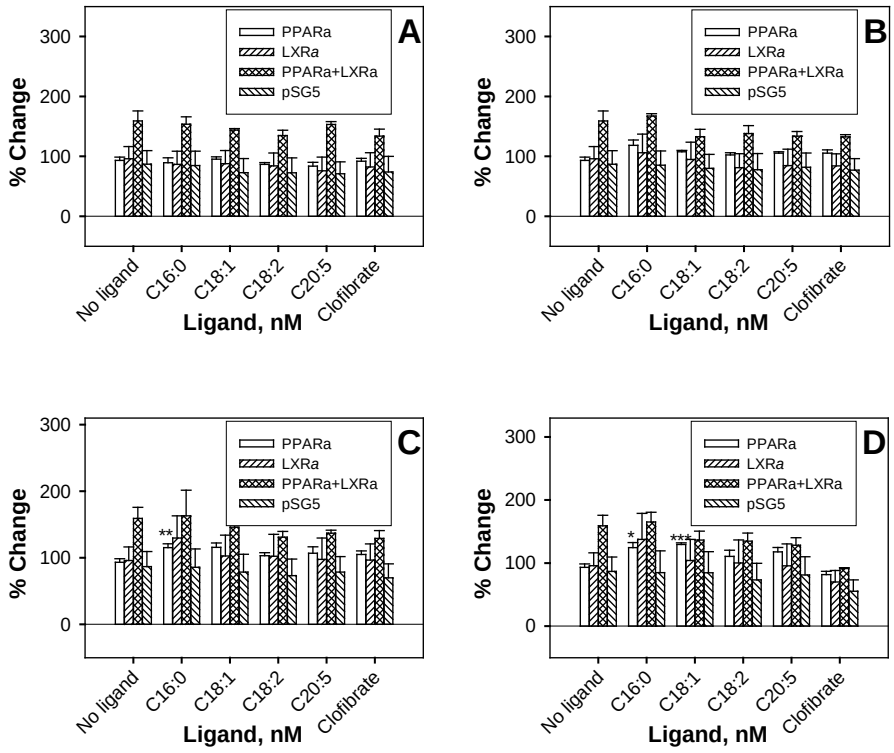

FIGURE 12: Transactivation of the PPARα regulated gene – ACOX in the absence and presence of different concentrations (1µM, 5µM, 10µM and 20µM) of fatty acids (palmitic acid, oleic acid, linoleic acid and EPA). The x-axis represents the different ligands plotted against the percentage change in activity of ACOX gene on y axis. **(A)** 1µM; **(B)** 5µM; **(C)** 10µM and **(D)** 20µM. Asterisks (*) represent significant differences due to different ligand concentrations as compared with the no-ligand for all the panels. *$p < 0.05$, **$p < 0.01$, ***$p < 0.001$.

To further examine the effects of the ligands on the LXR regulated gene – SREBP, the transactivation assay was repeated with an SREBP promoter upstream of luciferase gene in the presence and absence of all four ligands. For comparisons between PPARα and LXRα regulation, activity was measured by normalizing all values to the sample with ACOX and clofibrate. The cells treated with no ligand showed positive activity, with LXRα having the most activity and PPARα the least. Also, the activity of luciferase in cells transfected with PPARα (open bars) remained basal, and cells expressing LXRα (forward hash bars) showed an increased activity in all four groups tested with 1μM (Figure 13 A), 5μM (Figure 13 B), 10μM (Figure 13 C) and 20μM (Figure 13D) ligand concentration. However, in the presence of all four ligand concentrations, the cells transfected with both PPARα and LXRα showed decreased activity, indicating that PPARα could possibly play a role in down regulating LXRα genes at these given concentrations.

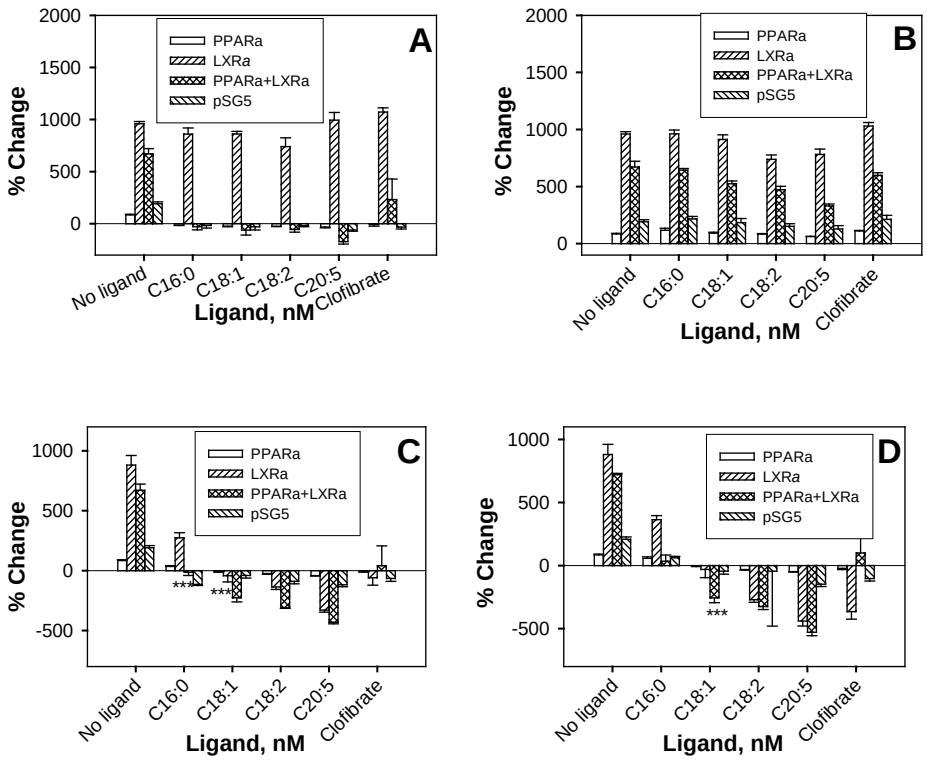

FIGURE 13: Transactivation of the LXRα regulated gene – SREBP in the absence and presence of different concentrations (1µM, 5µM, 10µM and 20µM) of fatty acids (palmitic acid, oleic acid, linoleic acid and EPA). The x-axis represents the different ligands plotted against the percentage change in activity of SREBP gene on y axis. **(A)** 1µM; **(B)** 5µM; **(C)** 10µM and **(D)** 20µM. Asterisks (*) represent significant differences due to different ligand concentrations as compared with the no-ligand for all the panels. *p < 0.05, **p < 0.01, ***p < 0.001.

V. DISCUSSION

PPARα and LXRα have been known to play a very important role in maintaining energy homeostasis and metabolism. As with any other protein, the stability and the function of a protein depends on its secondary structure, and therefore any change in the structural conformation may lead to an improper folding resulting in a change in its function. Similarly, with PPARα and LXRα, change in the structure or function of the protein may influence the normal functioning and result in an imbalance. It is therefore important to understand the effects of protein-protein or protein-ligand interaction on the structure and the function of the proteins. For example, PPARs have been known to bind LCFAs and LCFA-CoAs [39] and regulate genes involved in fatty acid metabolism by forming heterodimers with other nuclear receptors such as RXR [36, 62]. Similarly, the other nuclear receptor: LXR, activated by sterols is known to regulate cholesterol metabolism and dimerizes with its partner – RXR [52, 53].

While PPARα and LXRα have been known to communicate, and regulate each other's activity [54, 55], their direct interactions had not been completely elucidated. Furthermore, previous studies largely used either murine, tagged or truncated forms of these proteins [39, 63, 64]. Studies suggest that the truncated or tagged forms of nuclear receptors function differently when compared to the full length form, in terms of binding to ligand or recruitment of cofactors [65]. This study, therefore examined the ability of the two full-length proteins, hPPARα and hLXRα to directly interact with each other, and

to study the effects of several saturated and unsaturated fatty acids and their CoA thioesters on their interaction and function.

A circular dichroic spectrum of a mixture of recombinant, full-length human PPARα and LXRα showed a change in the secondary structure, and also suggested the possibility of an interaction. Fluorescent binding assays, further confirmed this interaction and for the first time showed high affinity binding of hPPARα and hLXRα with K_ds in the low nanomolar range. Furthermore, a coimmunoprecipitation assay using mouse liver homogenate showed that both PPARα and LXRα had the capacity to pull down the other protein further confirming the interaction of the two proteins *in vivo*. This interaction between the two proteins suggested that in addition to regulating each other indirectly (as suggested by Ide et. al) [2, 3], they could also interact directly and regulate genes involved in either fatty acid or cholesterol metabolism. The finding in this study opens up a galore of questions as to what pathway the heterodimer partners would regulate, and the factors governing the choice of the pathway they regulate.

Since ligand binding induces structural changes in these receptors, ligand binding may also alter protein-protein interactions and/or protein-DNA interactions, which could in turn alter gene regulation. This observation, and the finding that hPPARα and hLXRα directly interact, led to the second hypothesis that the known ligands for PPARα (fatty acids and their CoA thioesters) could play a role in the interaction of hPPARα and hLXRα. Therefore, circular dichroic spectral analysis of hPPARα and hLXRα as a

mixture and individually, were examined in the presence and absence of four different fatty acids and their CoA thioesters. Also, binding assays with a mixture of hPPARα and hLXRα were conducted in the presence of all four fatty acids and their CoA thioesters. While the CD spectral analysis showed changes in the secondary structure of the individual proteins in the presence of fatty acids and their CoAs, it suggested that the presence of such ligands could have an effect on the function as well. Although none of the examined ligands increased the interaction of hPPARα and hLXRα, several of the ligands had little or no effect, while others severely decreased the interaction of these proteins. This could suggest that in the presence of palmitic acid, oleic acid, oleoyl-CoA, and linoleoyl-CoA, hPPARα will readily heterodimerize with hLXRa – perhaps preferentially over hRXRα. For example, a mixture of hPPARα and hLXRα in the presence of palmitic acid (saturated) suggested that it does not interfere with the protein-protein interaction; further confirmed by binding studies that generated a K_d of 7±2nM, which is close to the binding affinity obtained in the absence of the ligands. This could mean that the presence of palmitic acid may not hinder hPPARα and hLXRα heterodimerization and also the metabolic pathway that they regulate. However, its CoA thioester – palmitoyl CoA showed a small decrease in binding (K_d of 53±17nM) correlating to the structural change observed on CD, which could have an effect on the downstream genes that PPARα or LXRα regulate. Moreover, since several of the examined ligands (linoleic, EPA, EPA-CoA) strongly decreased the affinity the proteins showed for each other, in the presence of these ligands, PPARα may prefer to bind to its other heterodimeric partner (RXRα), rather than LXRα. This choice of heterodimeric

partner could in turn determine which response elements will be bound, and in turn determine which pathways will be up or down regulated.

The transactivation assay data suggested that the four ligands – palmitic acid, oleic acid, linoleic acid and EPA did not significantly alter the expression of the PPARα-regulated gene ACOX in the presence of the heterodimer partner LXRα, suggesting that they might not affect fatty acid metabolism. It is however possible that the ligand concentrations used are not optimal for PPARα-LXRα activation, that LXRα might not be a preferred partner for heterodimerization in the presence of these fatty acids, or that PPARα heterodimerization to LXRα results in weaker binding to the PPRE of the acyl-CoA oxidase gene than when heterodimerized to RXRα (although still stronger than PPARα alone). On the other hand, cells transfected with the SREBP promoter showed a decrease in luciferase activity in the presence of both PPARα and LXRα indicating that the interaction of PPARα with LXRα decreases the expression of this LXRα-activated gene.

While saturated and unsaturated fatty acids are required by the body in moderate levels to perform normal functions, an excess will lead to imbalance. Previous studies have shown that the saturated fatty acid, palmitic acid is known to elevate cholesterol levels and also increase the risk of coronary heart diseases [66, 67]. However, these fatty acids are required to perform vital roles in lipogenesis, fat deposition and polyunsaturated fatty acids bioavailability in the cells [68]. In this current study, data from transactivation

assay shows that the presence of palmitic acid does not affect PPARα from interacting with LXRα. The results therefore indicate the possibility of PPAR-LXR heterodimer in decreasing LXRs ability to upregulate SREBP gene, which is involved in cholesterol metabolism. Therefore, palmitic acid decreases SREBP activity, and lowers cholesterol synthesis. Although the unsaturated fatty acids, oleic acid, linoleic acid and EPA affect PPARα and LXRα heterodimerization, they also decrease SREBP activity suggesting that a diet rich in fatty acids might help in reducing cholesterol. However, cholesterol is an important precursor to essential components such as steroids, vitamin D and bile. In the presence of high levels of cholesterol, PPARα-LXRα heterodimer is favored; however in presence of low levels of cholesterol, LXRα might preferentially bind to its partner RXR to activate cholesterol synthesis.

In summary, this is the first study to show not only direct interaction between full length human PPARα and LXRα, but also the effects of ligands on the binding and function of the two proteins.

LIST OF ABBREVIATIONS

ACOX - acyl-CoA oxidase

CPT1A - carnitine palmitoyl transferase 1A

DBD – DNA binding domain

DTT – Dithiothreitol

EDTA – Ethylene di amine tetra acetic acid

FAS – Fatty acyl synthase

FXR – Farsenoid X receptor

GLUT1 - glucose transporter

HRE – Hormone response elements

LBD – Ligand binding domain

LCFA – Long chain fatty acid

LCFA-CoA – Long chain fatty acyl CoA

L-FABP - liver-fatty acid binding protein

LXR – Liver X receptor

LXRE – Liver X receptor response elements

PPAR – peroxisome proliferator activated receptor

PPRE – peroxisome proliferator response elements

RXR – Retenoid X receptor

SDS – Sodium dodecyl sulphate

REFERENCES

1. Kung, H.C., et al., *Deaths: final data for 2005.* Natl Vital Stat Rep, 2008. **56**(10): p. 1-120.
2. Elizabeth, P., *Participation in occupation and diabetes self-management in emerging adulthood*. 2011.
3. Mangelsdorf, D.J., et al., *The nuclear receptor superfamily: the second decade.* Cell, 1995. **83**(6): p. 835-9.
4. Wahli, W. and E. Martinez, *Superfamily of steroid nuclear receptors: positive and negative regulators of gene expression.* FASEB J, 1991. **5**(9): p. 2243-9.
5. Hostetler, H.A., et al., *Glucose directly links to lipid metabolism through high affinity interaction with peroxisome proliferator-activated receptor alpha.* J Biol Chem, 2008. **283**(4): p. 2246-54.
6. Mitro, N., et al., *The nuclear receptor LXR is a glucose sensor.* Nature, 2007. **445**(7124): p. 219-23.
7. Parks, D.J., et al., *Bile acids: natural ligands for an orphan nuclear receptor.* Science, 1999. **284**(5418): p. 1365-8.
8. Enmark, E. and J.A. Gustafsson, *Orphan nuclear receptors--the first eight years.* Mol Endocrinol, 1996. **10**(11): p. 1293-307.
9. Mangelsdorf, D.J., et al., *Nuclear receptor that identifies a novel retinoic acid response pathway.* Nature, 1990. **345**(6272): p. 224-9.

10. Petkovich, M., et al., *A human retinoic acid receptor which belongs to the family of nuclear receptors.* Nature, 1987. **330**(6147): p. 444-50.

11. Blumberg, B. and R.M. Evans, *Orphan nuclear receptors--new ligands and new possibilities.* Genes Dev, 1998. **12**(20): p. 3149-55.

12. Laudet, V., *Evolution of the nuclear receptor superfamily: early diversification from an ancestral orphan receptor.* J Mol Endocrinol, 1997. **19**(3): p. 207-26.

13. Giguere, V., *Orphan nuclear receptors: from gene to function.* Endocr Rev, 1999. **20**(5): p. 689-725.

14. BARRY MARC FORMAN, R.M., *Nuclear Hormone Receptors Activate Direct, Inverted, and Everted Repeats.* Annals of the New York Academy of Sciences, 2006. **761**: p. 29-37.

15. Aranda, A. and A. Pascual, *Nuclear hormone receptors and gene expression.* Physiol Rev, 2001. **81**(3): p. 1269-304.

16. Berg, J.M., *DNA binding specificity of steroid receptors.* Cell, 1989. **57**(7): p. 1065-8.

17. Cronet, P., et al., *Structure of the PPARalpha and -gamma ligand binding domain in complex with AZ 242; ligand selectivity and agonist activation in the PPAR family.* Structure, 2001. **9**(8): p. 699-706.

18. Nolte, R.T., et al., *Ligand binding and co-activator assembly of the peroxisome proliferator-activated receptor-gamma.* Nature, 1998. **395**(6698): p. 137-43.

19. Weatherman, R.V., R.J. Fletterick, and T.S. Scanlan, *Nuclear-receptor ligands and ligand-binding domains.* Annu Rev Biochem, 1999. **68**: p. 559-81.

20. Xu, H.E., et al., *Structural determinants of ligand binding selectivity between the peroxisome proliferator-activated receptors.* Proc Natl Acad Sci U S A, 2001. **98**(24): p. 13919-24.

21. Svensson, S., et al., *Crystal structure of the heterodimeric complex of LXRalpha and RXRbeta ligand-binding domains in a fully agonistic conformation.* EMBO J, 2003. **22**(18): p. 4625-33.

22. Vincent Laudet, J.A., Jan- and A.G.a.W. Wahli, *A unified nomenclature system for the nuclear receptor superfamily.* Cell, 1999. **97**(2): p. 161-3.

23. de Duve, C., *The peroxisome: a new cytoplasmic organelle.* Proc R Soc Lond B Biol Sci, 1969. **173**(30): p. 71-83.

24. Issemann, I. and S. Green, *Activation of a member of the steroid hormone receptor superfamily by peroxisome proliferators.* Nature, 1990. **347**(6294): p. 645-50.

25. Kliewer, S.A., et al., *Peroxisome proliferator-activated receptors: from genes to physiology.* Recent Prog Horm Res, 2001. **56**: p. 239-63.

26. Boitier, E., J.C. Gautier, and R. Roberts, *Advances in understanding the regulation of apoptosis and mitosis by peroxisome-proliferator activated receptors in pre-clinical models: relevance for human health and disease.* Comp Hepatol, 2003. **2**(1): p. 3.

27. Kersten, S., et al., *Peroxisome proliferator-activated receptor alpha mediates the adaptive response to fasting.* J Clin Invest, 1999. **103**(11): p. 1489-98.

28. Leone, T.C., C.J. Weinheimer, and D.P. Kelly, *A critical role for the peroxisome proliferator-activated receptor alpha (PPARalpha) in the cellular fasting response: the PPARalpha-null mouse as a model of fatty acid oxidation disorders.* Proc Natl Acad Sci U S A, 1999. **96**(13): p. 7473-8.

29. Chawla, A., et al., *Peroxisome proliferator-activated receptor (PPAR) gamma: adipose-predominant expression and induction early in adipocyte differentiation.* Endocrinology, 1994. **135**(2): p. 798-800.

30. Devchand, P.R., et al., *The PPARalpha-leukotriene B4 pathway to inflammation control.* Nature, 1996. **384**(6604): p. 39-43.

31. Finck, B.N., et al., *A potential link between muscle peroxisome proliferator-activated receptor-alpha signaling and obesity-related diabetes.* Cell Metab, 2005. **1**(2): p. 133-44.

32. Lehmann, J.M., et al., *An antidiabetic thiazolidinedione is a high affinity ligand for peroxisome proliferator-activated receptor gamma (PPAR gamma).* J Biol Chem, 1995. **270**(22): p. 12953-6.

33. Forman, B.M., et al., *15-Deoxy-delta 12, 14-prostaglandin J2 is a ligand for the adipocyte determination factor PPAR gamma.* Cell, 1995. **83**(5): p. 803-12.

34. Krey, G., et al., *Fatty acids, eicosanoids, and hypolipidemic agents identified as ligands of peroxisome proliferator-activated receptors by coactivator-dependent receptor ligand assay.* Mol Endocrinol, 1997. **11**(6): p. 779-91.

35. Holden, P.R. and J.D. Tugwood, *Peroxisome proliferator-activated receptor alpha: role in rodent liver cancer and species differences.* J Mol Endocrinol, 1999. **22**(1): p. 1-8.

36. Kliewer, S.A., et al., *Convergence of 9-cis retinoic acid and peroxisome proliferator signalling pathways through heterodimer formation of their receptors.* Nature, 1992. **358**(6389): p. 771-4.

37. Juge-Aubry, C.E., et al., *Peroxisome proliferator-activated receptor mediates cross-talk with thyroid hormone receptor by competition for retinoid X receptor. Possible role of a leucine zipper-like heptad repeat.* J Biol Chem, 1995. **270**(30): p. 18117-22.

38. Escher, P. and W. Wahli, *Peroxisome proliferator-activated receptors: insight into multiple cellular functions.* Mutat Res, 2000. **448**(2): p. 121-38.

39. Hostetler, H.A., et al., *Peroxisome proliferator-activated receptor alpha interacts with high affinity and is conformationally responsive to endogenous ligands.* J Biol Chem, 2005. **280**(19): p. 18667-82.

40. Poirier, Y., et al., *Peroxisomal beta-oxidation--a metabolic pathway with multiple functions.* Biochim Biophys Acta, 2006. **1763**(12): p. 1413-26.

41. Francis, G.A., et al., *Nuclear receptors and the control of metabolism.* Annu Rev Physiol, 2003. **65**: p. 261-311.

42. Tontonoz, P. and D.J. Mangelsdorf, *Liver X receptor signaling pathways in cardiovascular disease.* Mol Endocrinol, 2003. **17**(6): p. 985-93.

43. Peet, D.J., B.A. Janowski, and D.J. Mangelsdorf, *The LXRs: a new class of oxysterol receptors.* Curr Opin Genet Dev, 1998. **8**(5): p. 571-5.

44. Janowski, B.A., et al., *An oxysterol signalling pathway mediated by the nuclear receptor LXR alpha.* Nature, 1996. **383**(6602): p. 728-31.

45. Lehmann, J.M., et al., *Activation of the nuclear receptor LXR by oxysterols defines a new hormone response pathway.* J Biol Chem, 1997. **272**(6): p. 3137-40.

46. Auboeuf, D., et al., *Tissue distribution and quantification of the expression of mRNAs of peroxisome proliferator-activated receptors and liver X receptor-alpha in humans: no alteration in adipose tissue of obese and NIDDM patients.* Diabetes, 1997. **46**(8): p. 1319-27.

47. Willy, P.J., et al., *LXR, a nuclear receptor that defines a distinct retinoid response pathway.* Genes Dev, 1995. **9**(9): p. 1033-45.

48. Apfel, R., et al., *A novel orphan receptor specific for a subset of thyroid hormone-responsive elements and its interaction with the retinoid/thyroid hormone receptor subfamily.* Mol Cell Biol, 1994. **14**(10): p. 7025-35.

49. Stulnig, T.M., et al., *Novel roles of liver X receptors exposed by gene expression profiling in liver and adipose tissue.* Mol Pharmacol, 2002. **62**(6): p. 1299-305.

50. Faulds, M.H., C. Zhao, and K. Dahlman-Wright, *Molecular biology and functional genomics of liver X receptors (LXR) in relationship to metabolic diseases.* Curr Opin Pharmacol. **10**(6): p. 692-7.

51. Fowler, A.J., et al., *Liver X receptor activators display anti-inflammatory activity in irritant and allergic contact dermatitis models: liver-X-receptor-specific*

inhibition of inflammation and primary cytokine production. J Invest Dermatol, 2003. **120**(2): p. 246-55.

52. Repa, J.J., et al., *Regulation of mouse sterol regulatory element-binding protein-1c gene (SREBP-1c) by oxysterol receptors, LXRalpha and LXRbeta.* Genes Dev, 2000. **14**(22): p. 2819-30.

53. Schultz, J.R., et al., *Role of LXRs in control of lipogenesis.* Genes Dev, 2000. **14**(22): p. 2831-8.

54. Yoshikawa, T., et al., *Cross-talk between peroxisome proliferator-activated receptor (PPAR) alpha and liver X receptor (LXR) in nutritional regulation of fatty acid metabolism. I. PPARs suppress sterol regulatory element binding protein-1c promoter through inhibition of LXR signaling.* Mol Endocrinol, 2003. **17**(7): p. 1240-54.

55. Ide, T., et al., *Cross-talk between peroxisome proliferator-activated receptor (PPAR) alpha and liver X receptor (LXR) in nutritional regulation of fatty acid metabolism. II. LXRs suppress lipid degradation gene promoters through inhibition of PPAR signaling.* Mol Endocrinol, 2003. **17**(7): p. 1255-67.

56. Petrescu, A.D., et al., *Structural and functional characterization of a new recombinant histidine-tagged acyl coenzyme A binding protein (ACBP) from mouse.* Protein Expr Purif, 2008. **58**(2): p. 184-93.

57. Hostetler, H.A., et al., *L-FABP directly interacts with PPAR alpha in cultured primary hepatocytes.* Journal of Lipid Research, 2009. **50**(8): p. 1663-1675.

58. Sreerama, N., S.Y. Venyaminov, and R.W. Woody, *Estimation of protein secondary structure from circular dichroism spectra: inclusion of denatured proteins with native proteins in the analysis.* Anal Biochem, 2000. **287**(2): p. 243-51.

59. Spector, A.A. and J.C. Hoak, *An improved method for the addition of long-chain free fatty acid to protein solutions.* Anal Biochem, 1969. **32**(2): p. 297-302.

60. Luci, S., et al., *Clofibrate causes an upregulation of PPAR-{alpha} target genes but does not alter expression of SREBP target genes in liver and adipose tissue of pigs.* Am J Physiol Regul Integr Comp Physiol, 2007. **293**(1): p. R70-7.

61. Horton, J.D., J.L. Goldstein, and M.S. Brown, *SREBPs: activators of the complete program of cholesterol and fatty acid synthesis in the liver.* J Clin Invest, 2002. **109**(9): p. 1125-31.

62. Hellemans K, K.K., Hannaert JC, Martens G, Van Veldhoven P, Pipeleers D., *Peroxisome proliferator-activated receptor alpha-retinoid X receptor agonists induce beta-cell protection against palmitate toxicity.* The FEBS Journal, 2007. **274**(23): p. 6094-6105.

63. Hostetler, H.A., A.B. Kier, and F. Schroeder, *Very-long-chain and branched-chain fatty acyl-CoAs are high affinity ligands for the peroxisome proliferator-activated receptor alpha (PPARalpha).* Biochemistry, 2006. **45**(24): p. 7669-81.

64. Hostetler, H.A., et al., *Glucose regulates fatty acid binding protein interaction with lipids and peroxisome proliferator-activated receptor alpha.* J Lipid Res, 2010. **51**(11): p. 3103-16.

65. Tian, H., et al., *The N-Terminal A/B domain of the thyroid hormone receptor-beta2 isoform influences ligand-dependent recruitment of coactivators to the ligand-binding domain.* Mol Endocrinol, 2006. **20**(9): p. 2036-51.

66. Connor, W.E., *Harbingers of coronary heart disease: dietary saturated fatty acids and cholesterol. Is chocolate benign because of its stearic acid content?* Am J Clin Nutr, 1999. **70**(6): p. 951-2.

67. Daan Kromhout, B.B., Edith Feskens, Alessandro Menotti, Aulikki Nissinen, *Saturated fat, vitamin C and smoking predict long-term population all-cause mortality rates in the seven countries study*

International Journal of Epidemiology, 2000. **29**: p. 260 - 265.

68. Philippe Legrand, V.R., *The Complex and Important Cellular and Metabolic Functions of Saturated Fatty Acids*

Lipids, 2010. **45**: p. 941–946.